RESEARCH ARTICLE

Human Mutation

OFFICIAL JOURNAL
HGVS
HUMAN GENOME VARIATION SOCIETY
www.hgvs.org

Microarray-Based Copy Number Analysis of Neurofibromatosis Type-1 (NF1)-Associated Malignant Peripheral Nerve Sheath Tumors Reveals a Role for Rho–GTPase Pathway Genes in NF1 Tumorigenesis

Meena Upadhyaya,[1]* Gill Spurlock,[1] Laura Thomas,[1] Nick S. T. Thomas,[1] Mark Richards,[1] Viktor-Felix Mautner,[2] David N. Cooper,[1] Abhijit Guha,[3]† and Jim Yan[4]

[1] *Institute of Medical Genetics, School of Medicine, Cardiff University, Cardiff, UK;* [2] *Department of Neurosurgery, University Clinic Hamburg-Eppendorf, Hamburg, Germany;* [3] *The Arthur and Sonia Labatt Brain Tumor Research Centre, The Hospital for Sick Children, University of Toronto, Toronto, Ontario, Canada;* [4] *Companion Diagnostics, Laboratory Corporation of America, Yorkshire Place, Durham, North Carolina*

Communicated by Paolo M. Fortina

Received 5 October 2011; accepted revised manuscript 18 January 2012.
Published online 13 February 2012 in Wiley Online Library (www.wiley.com/humanmutation).DOI: 10.1002/humu.22044

ABSTRACT: Neurofibromatosis type-1 (NF1) is associated with the growth of benign and malignant tumors. Approximately 15% of NF1 patients develop malignant peripheral nerve sheath tumors (MPNSTs), underlining the need to identify specific diagnostic/prognostic biomarkers associated with MPNST development. The Affymetrix Genome-Wide Human single-nucleotide polymorphism (SNP) Array 6.0 was used to perform SNP genotyping and copy number alteration (CNA), loss-of-heterozygosity (LOH), and copy number neutral–LOH (CNN–LOH) analyses of DNA isolated from 15 MPNSTs, five benign plexiform neurofibromas (PNFs), and patient-matched lymphocyte DNAs. MPNSTs exhibited high-level CNN-LOH, with recurrent changes occurring in MPNSTs but not PNFs. CNN–LOH was evident in MPNSTs but occurred less frequently than genomic deletions. CNAs involving the *ITGB8*, *PDGFA*, Ras-related C3 botulinum toxin substrate 1 (*RAC1*) (7p21-p22), *PDGFRL* (8p22-p21.3), and matrix metallopeptidase 12 (*MMP12*) (11q22.3) genes were specific to MPNSTs. Pathway analysis revealed the MPNST-specific amplification of seven Rho–GTPase pathway genes and several cytoskeletal remodeling/cell adhesion genes. In knockdown experiments employing short-hairpin *RAC1*, *ROCK2*, *PTK2*, and *LIMK1* RNAs to transfect both control and MPNST-derived cell lines, cell adhesion was significantly increased in the MPNST cell lines, whereas wound healing, cell migration, and invasiveness were reduced, consistent with a role for these Rho–GTPase pathway genes in MPNST development and metastasis. These results suggest new targets for therapeutic intervention in relation to MPNSTs.

Hum Mutat 33:763–776, 2012.

KEY WORDS: neurofibromatosis type-1; benign and malignant tumors; loss-of-heterozygosity; copy number alterations; Rho–GTPase pathway genes; cell adhesion; migration; invasion; wound healing; metastasis

Introduction

Neurofibromatosis type-1 (NF1; MIM# 162200) is a familial cancer syndrome that affects one in 3,500 individuals worldwide. It is caused by inactivation of the *NF1* tumor suppressor gene (MIM# 162200) located at 17q11.2. Consistent with Knudson's two-hit hypothesis, NF1 patients harboring a heterozygous germline *NF1* mutation develop neurofibromas upon somatic mutation of the second wild-type *NF1* allele. The benign and malignant peripheral nerve sheath tumors (MPNSTs) that develop in NF1 patients are a hallmark of the disease, with cutaneous neurofibromas being the commonest benign tumors, and MPNSTs, a type of sarcoma, contributing to malignancy [Bennett et al., 2009; Upadhyaya and Cooper, 1998; reviewed by Upadhyaya, 2010]. NF1 individuals are predisposed to develop a variety of other cancers, such as optic gliomas, pheochromocytomas, gastrointestinal stromal tumors, and myeloid malignancies. NF1 is also characterized by a plethora of nontumor clinical features, including dermal pigmentary changes, hamartomatous lesions of the iris, bone deformities, and cognitive deficit.

Neurofibromatosis type-1 patients exhibit an 8–13% lifetime risk of developing an MPNST, usually from within a preexisting plexiform neurofibroma (PNF) or a focal subcutaneous neurofibroma [Brems et al., 2009a; Evans et al., 2002; Spurlock et al., 2010; Tucker et al., 2005 & Carrolle & Ratner, 2008]. Although most MPNSTs develop in adult NF1 patients, they can also occur in much younger affected individuals, emphasizing the need for early detection of MPNST development given that these aggressive tumors frequently recur and can metastasize to the lungs and other organs. Radical

Additional Supporting Information may be found in the online version of this article.

†This manuscript is dedicated to the memory of Professor Abhijit Guha, who sadly passed away on 8 November 2011, shortly before this article was accepted for publication.

*Correspondence to: Meena Upadhyaya, Institute of Medical Genetics, School of Medicine, Cardiff University, Cardiff CF14 4XN, UK. E-mail: upadhyaya@cardiff.ac.uk

surgery, usually in combination with radiotherapy, constitutes the optimum treatment, especially if chemotherapy is also given in parallel to inhibit metastasis. Although early detection would facilitate both the identification and clinical management of those NF1 patients most likely to develop malignant tumors, a prerequisite for early detection is the availability of diagnostic and prognostic biomarkers associated with MPNST development [reviewed by Upadhyaya, 2011].

The difficulties inherent in the early clinical and pathological diagnosis of NF1–MPNSTs underline the need for a clearer definition of the molecular basis of NF1-associated malignancy. Somatic biallelic inactivation of both *NF1* alleles was first demonstrated in NF1–MPNSTs more than 20 years ago [Skuse et al., 1989], an observation consistent with *NF1* being a tumor suppressor gene. Homozygous *NF1* inactivation was also subsequently detected in benign cutaneous and PNFs as well as in MPNSTs when loss-of-heterozygosity (LOH) analysis was performed [Glover et al., 1991; John et al., 2000; Legius et al., 1993; Rasmussen et al., 2000], indicating that additional genetic changes are required for malignant transformation to occur.

Although the functional loss of neurofibromin represents the primary event in tumorigenesis, the precise role of other genetic lesions in promoting the malignant transformation of benign neurofibromas is poorly understood. However, the recent introduction of microarray-based technologies allows us to simultaneously analyze multiple genes and genomic regions (at both the RNA and DNA level) in a single experiment. Such array-based analyses provide us with an unrivaled opportunity to profile concomitant copy number and gene expression changes associated with a given tumor state. Several studies have already analyzed tumor DNA and/or RNA in searches for potential molecular signatures capable of differentiating between MPNSTs and benign neurofibromas [Miller et al., 2006, 2010; Mantripragada et al., 2008, 2009; reviewed by Upadhyaya, 2011]. Array-based analyses have a major advantage in that they can be used to detect copy number variation/alterations, which can play a key role in tumorigenesis. Copy number variants (CNVs) constitute heritable genomic alterations that range in size from one kilobase up to several megabases in size. Although CNVs make a substantial contribution to interindividual variation, acquired somatic copy number alterations (CNAs) are increasingly being identified in many different cancers [Albertson, 2006; Kuiper et al., 2010; Rothenberg and Settleman, 2010; Shlien and Malkin, 2009, 2010]. As with other tumor-associated genetic changes, such CNAs (by virtue of the genes they contain) can confer a selective advantage with respect to cellular proliferation, survival, and clonal expansion. Various microarray-based methodologies have been developed to detect both CNVs and CNAs genome wide. Initially, comparative genomic hybridization arrays (array-CGH) constructed from overlapping human bacterial artificial chromosome (BAC) clones were recruited, but more recently, combined high-density single-nucleotide polymorphism (SNP) and CNV genotyping arrays have been employed. Such high-density microarrays, often containing several million individual markers, can now be used to simultaneously assess both heritable copy number variation and somatic CNA-based genomic changes associated with a specific tumor type [Lebron et al., 2011].

Recent studies of NF1-associated benign and malignant tumors, which have aimed to identify tumor-specific diagnostic and prognostic markers, have detected extensive somatic copy number changes in DNA derived from NF1–MPNSTs that were absent from the DNA of benign PNFs [Kresse et al., 2008; Mantripragada et al., 2008, 2009]. The present study has extended this analysis by providing high-resolution information from a combined genomic CNA analysis with data from an LOH screen of both PNF and MPNST tumor DNAs from 20 unrelated NF1 patients using the Affymetrix Genome-Wide Human SNP 6.0 Array.

Materials and Methods

Patient Samples and DNA Preparation

This project was approved by the local Ethics committee. Informed consent for sample collection was obtained according to protocols approved by this committee. Diagnosis of MPNSTs was made by the individual referring centers. All available information on the nature and grading of the tumors under study (15 MPNSTs) is provided in Supp. Table S1. Tumor biopsies and matched lymphocyte samples were obtained from the 20 unrelated NF1 patients. DNA from the tumors and matched lymphocyte samples was extracted as previously described [Upadhyaya et al., 2008a, 2008b]. DNA samples were checked to ensure compliance with the stringent spectrophotometric and electrophoretic quality control (QC) criteria required by the Affymetrix SNP 6.0 Array platform.

Affymetrix SNP 6.0 Array Analysis

The Affymetrix Genome-Wide Human SNP Array 6.0 was used as per the manufacturer's instructions. This Affymetrix array offers whole-genome coverage as well as superior resolution, and permits the simultaneous assessment of unbalanced chromosomal defects such as CNA, LOH, and acquired copy number neutral (CNN)–LOH. Details are given in the Supp. Methods.

Genomic Segmentation algorithms or Hidden Markov Model (HMM) (Affymetrix White Paper; http://www.affymetrix.com/support/technical/whitepapers.affx) were used to detect the copy number variation. The minimal number of genomic markers was set at 50 for both algorithms. Most copy number analysis was performed using the segmentation method, with the *P* value threshold set at 0.001 and a signal-to-noise ratio of ≥0.5, to attain the level required for positive CNA detection. In these copy number analyses, overlapping CNA regions were identified on the basis of the overlap of physical location intervals at each CNA boundary, either in NF1–MPNSTs or benign PNFs. All CNA and LOH analyses, including CNN–LOH, were performed in Partek Genomics Suite 6.4. Most CNA analysis entailed paired analysis involving the comparison of tumor DNAs against the matched constitutional patient lymphocyte DNAs, whereas unpaired CNA analysis was only used in median absolute pairwise difference (MAPD) calculation and QC to compare tumor DNA against reference data derived from the 270 normal individuals catalogued in the HapMap database (International HapMap Consortium, 2005). All LOH and CNN–LOH analyses were paired using matched lymphocyte DNAs as the baseline. Each positive tumor-specific CNA was assessed to determine the genomic region, overlap, or recurrence between samples, as well as the identity of the genes residing within the corresponding genomic regions. For CNN–LOH analysis, two separate workflows were used. One of these was the allele-specific copy number (ASCN) analysis in Partek that used both the CEL files containing probe intensity data and CHP files containing SNP call results together to assess copy number allele imbalance. The other workflow involved the comparison of paired CNV analysis using CEL files and paired LOH analysis (using both CEL files and CHP files) to identify regions with CNVs and LOH, respectively, and then to identify regions of CNN–LOH. The results from the two separate workflows were then merged, generating a consensus in CNN–LOH identification. Biological pathway analysis was performed in GeneGO's MetaCore (http://www.genego.com)

using gene set enrichment analysis in conjunction with the gene lists from the corresponding CNA regions or LOH regions.

Quantitative Real-Time Polymerase Chain Reaction

From the derived Affymetrix array CGH data in the present study, the relative copy numbers of 14 genes found to be encompassed by tumor-specific CNAs were independently assessed by quantitative polymerase chain reaction (qPCR) of DNA and RNA isolated from the relevant tumor samples. The details are given in the Supporting Information.

Details of the short-hairpin RNA (shRNA) experiments, cell culture, Western blotting, immunohistochemistry, the wound healing assay, and the cell adhesion, invasion, and migration assays are given in the Supporting Information.

Results

Data Quality Assessment

In the present study, we analyzed the copy number and LOH state in DNA isolated from tumors and matched constitutional (lymphocyte) samples from 20 NF1 patients (including 15 MPNSTs and five PNFs) using the Affymetrix 6.0 SNP array. (NB. Throughout the text, the prefix M denotes MPNST, whereas the prefix P denotes PNF.) Because LOH and CNN–LOH analyses require satisfactory genotyping performance and consistent intensity measurement across genomic regions, we examined the SNP call rate to assess genotyping performance, MAPD to assess the suitability for using unpaired copy number analysis against the 794 normal HapMap samples (Supp. Fig. S1a–c), and principal component analysis (PCA) and clustering analysis for sample grouping and detection of sample outliers. Apart from one lymphocyte sample (patient M6) that failed to yield DNA of sufficient quality, all 39 samples successfully yielded data. The SNP call rates for 36 of the 39 arrays analyzed were 97–99%, and were therefore suitable for LOH analysis. The remaining three arrays yielded SNP call rates of 96.0–96.8% with acceptable genotyping performance and were therefore also included in the data analysis. All 39 DNA hybridizations yielded good MAPD scores, 0.23–0.37 (<0.4), thereby meeting the acceptance criterion for copy number analysis.

The clustering analysis (Fig. 1a and b) of copy numbers from the unpaired and paired analyses indicated that the MPNSTs represented a diverse group, with some samples (M10, M11, M12, M13, and M14) resembling PNF samples in terms of their copy number changes, whereas others (such as M2, M3, M7, M8, M9, and MX) were quite distinct from the PNF samples. After reviewing the PCA and clustering analysis results of copy numbers from the unpaired analysis, an apparent batch effect related to scan date (data production date) was noted. Three arrays, corresponding to M14 tumor and lymphocyte samples and M9 tumor samples produced on September 16, 2008 (Supp. Fig. S1a) deviated significantly from the rest of data due to the scan date batch effect. Although the paired analysis (Fig. 1a) placed M14 in the middle of the cluster, because both its tumor and matched lymphocyte samples were from the same batch, M9 would appear to be an outlier in the paired analysis because its tumor sample was profiled in the batch of September 16, 2008, but its matched reference lymphocyte sample was made in the other batch (August 28, 2008). Therefore, M9 was not used for any sample overlap and recurrent CNA analysis.

The genome-wide CNA/CNV profiles associated with each tumor type and the matching lymphocyte DNA from the same patient were visualized using the heatmaps generated from hierarchical clustering analysis in Partek Genomics Suite 6.4. Each CNA profile was presented as a "heatmap" that depicted the copy number changes associated with each of the 23 chromosomes. As an example, the CNA heatmap for chromosome 5 is shown for the 13 MPNST tumor samples (top panel) and five PNF tumor samples pairwise in Figure 2; this serves to identify all copy number gains (in red) and all copy number losses (in blue) across the entire length of chromosome 5. Five PNF-harboring patients (bottom panel) displayed relatively few copy number changes, whereas the CNA profiles derived from five MPNSTs (top panel, M2, M3, M5, M6, M7, M8, and MX) were generally comparable (with genomic gains across the entire 5p arm and genomic losses across the 5q arm). However, the CNA profiles from several other MPNSTs (M4, M10, M11, M12, and M13) were quite varied, with several displaying CNA profiles with respect to chromosome 5 that were similar to those exhibited by benign PNFs. The genome-wide CNA profiles associated with the MPNSTs displayed a similar trend; however, these molecular profiles harbored two subgroups of malignant tumors, those that exhibited a large number of CNAs and those which exhibited relatively few CNA profiles and were comparable to the profiles characterizing benign PNFs (Figs. 1a and 2).

CNV/CNA Identification by Paired and Unpaired Analysis

To determine whether any of the identified CNAs were specific to either the PNFs or the malignant MPNSTs, all tumor CNVs/CNAs were compared with the CNV profiles derived from the matched lymphocyte DNA samples from the same patients, as well as against the CNV profiles of the 794 normal HapMap samples. The Database of Genomic Variants (http://projects.tcag.ca/variation/) was queried for all CNV/CNA-harboring regions identified in the tumor and blood samples in order to exclude the possibility that they might constitute rare CNVs found in the normal population rather than true somatic events. To identify significant CNAs, we employed the criteria of 50 or more markers, a P value of 0.001 and a signal-to-noise ratio of no less than 0.5 for segmentation analysis. The CNA distributions in 14 MPNST and five PNF patients are summarized in Table 1 and Supp. Tables S2 and S3 for both the paired and unpaired analyses. The detailed results for individual patients are presented in Supp. Table S4. It would appear that CNAs in MPNSTs are much more frequent than in PNFs in the paired analysis (Table 1, Supp. Fig. S2a and b). The unpaired analysis yielded more CNAs in some samples than the paired analysis (Table 1), indicating that germline CNVs were evident in the unpaired analysis but not in the paired analysis. These results from the unpaired analysis did not include the X and Y chromosomes because the genders of individuals from the HapMap samples were different from those of the NF1 patients and hence inclusion of the sex chromosomes would have rendered the CNA analysis invalid. Therefore, the primary results and conclusion were based solely on the paired analysis. The unpaired analysis was mainly used to assess the difference between the somatic and germline changes. Among the results of the paired analysis, 41 CNAs had copy numbers greater than 4 or less than 0.5; 40 of these high-magnitude changes occurred in MPNST patients M2, M3, M7, M8, and MX including 13 amplifications on 18q21.2 in patient M3, two deletions on 17p11.2 in patient M2, and three deletions on 11p12 in MX. Only one amplification event was found in a PNF (P1 on 12p11.1).

Deletions and Amplifications

Of the total 1,022 CNVs/CNAs identified, there were more copy number losses (571; 55.87%) than copy number gains (451;

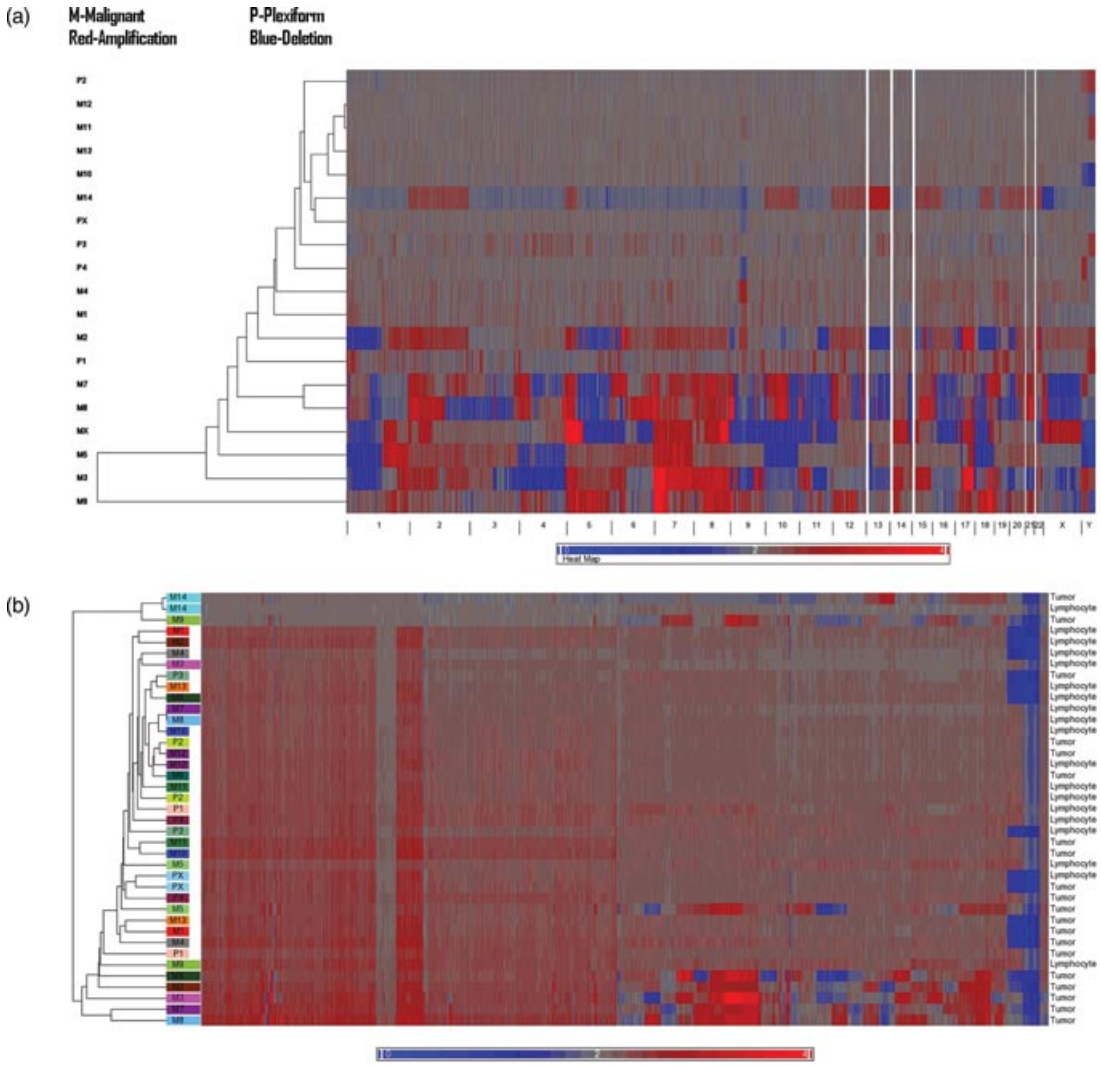

Figure 1. (A) Hierachical clustering of genome-wide copy number from the paired analysis. Global clustering view of copy number alterations across all NF1 tumor samples. M, malignant; P, plexiform neurofibromas amplification is indicated by red and deletion is denoted by blue. (B) Hierachical clustering of genome-wide copy number from the unpaired analysis compared with the HapMap reference. Amplification is indicated by red and deletion is denoted by blue.

44.13%). Most CNAs (996/1022) were identified in MPNST tumor DNA, whereas only 26 CNAs were identified in benign PNF tumor DNA (Supp. Table S3). Recurrent or overlapping CNVs/CNAs were absent from PNFs (Supp. Table S3), except for one overlap on chromosome 4 in two patients, P1 and P3. Identification of the CNAs most likely to be involved in malignant transformation required the selection of recurrent CNAs (i.e., those CNAs found in at least three different MPNSTs from unrelated patients, and with copy number gains of ≥2.8 or losses of ≤1.5); employing these criteria, a total of 232 CNVs were selected for further analysis (all were among the MPNSTs because no such recurrent CNAs were observed among the benign PNFs). A subsequent assessment of the 232 recurrent MPNST-associated CNAs identified at least 2,972 genes that were contained within, or overlapped with, these variant genomic regions (Supp. Table S4, overlapping genes).

LOH Analysis and CNN–LOH analysis

The 19 pairs of samples were used to identify regions with CNN changes. Patient M6 was excluded owing to the lack of sufficient matched lymphocyte sample. In LOH analysis, a matched reference is required to eliminate potentially confounding genotypic differences from the reference sample. Two approaches were used to identify CNN changes (uniparental disomy) using Partek Genomics Suite 6.4. First, CNN–LOH was analyzed to identify regions where LOH was identified, yet total copy number equalled 2. Second, the ASCN was performed to identify CNN allele imbalance.

The 19 pairs of samples (corresponding to DNAs from 14 MPNSTs and five PNFs) were used in LOH analysis with the individually matched lymphocyte DNAs serving as reference samples in the paired analysis (Table 2).

Loss-of-heterozygosity results were obtained from paired analyses of matched tumor and lymphocyte DNAs from each patient using the SNP probe set in the Affymetrix SNP6.0 array. MPNST DNAs exhibited a higher level of LOH (with a considerable number of overlapping regions) as compared with benign tumors.

In total, 7,643 LOH regions were found that exhibited a heterozygosity rate of zero for at least two SNP markers. Supp. Table S3 summarizes the results obtained in LOH analysis and illustrates the very high levels of LOH exhibited by MPNST DNA as compared

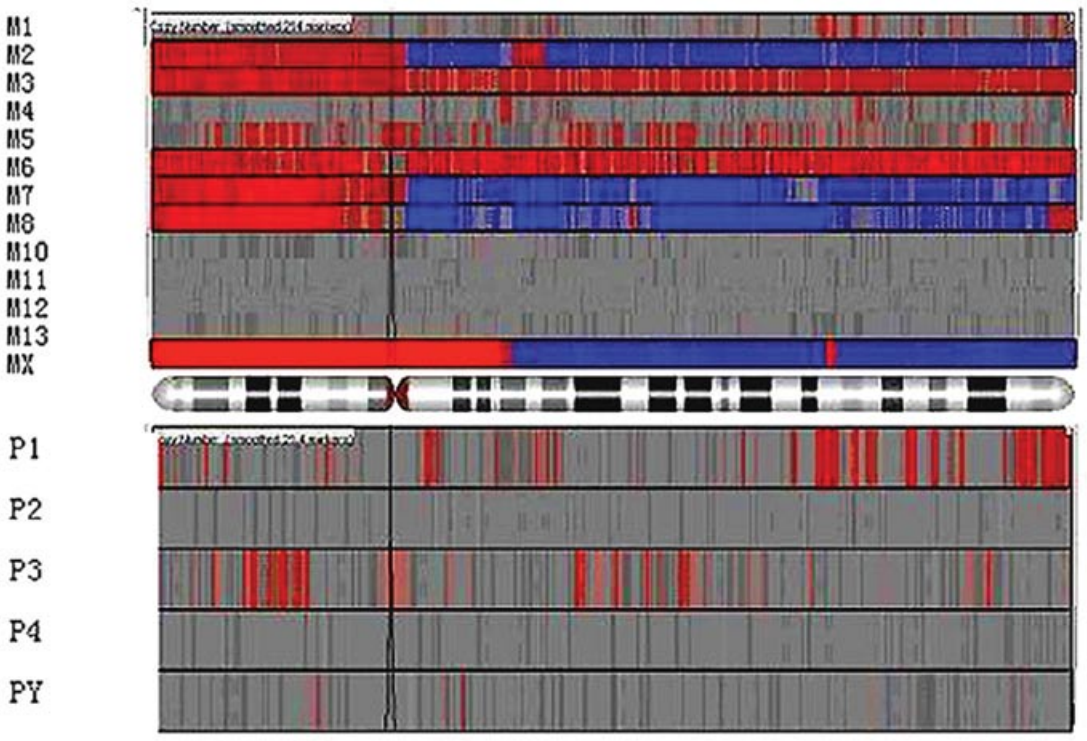

Figure 2. Copy number alteration (CNA) analysis of all NF1 tumor samples, both benign PNFs and malignant MPNSTs for chromosome 5. CNA heatmap for chromosome 5 is shown for the 13 MPNST tumor samples (top panel) and five PNF tumor samples pairwise; it identifies all copy number gains (in red) and all copy number losses (in blue) across the entire length of chromosome 5. Five PNF-harboring patients (bottom panel) displayed relatively few copy number changes, whereas the CNA profiles derived from five MPNSTs (top panel, M2, M3, M5, M6, M7, M8, and MX) were generally comparable (with genomic gains across the entire 5p arm and genomic losses across the 5q arm). However, the CNA profiles from several other MPNSTs (M4, M10, M11, M12, and M13) were quite varied, with several displaying CNA profiles with respect to chromosome 5 that were similar to those exhibited by benign PNFs.

with the general lack of LOH, evident in benign PNF tumor DNAs. Among the MPNST DNA samples, a considerable number of overlapping LOH regions were observed, with at least 450 overlapping regions identified in five tumors and 40 overlapping regions identified in six tumors. In contrast, no overlap in LOH was found among the benign PNF tumors. In the paired copy number analysis, the 19 pairs of samples were used in HMM copy number analysis using their matched lymphocyte samples as a reference and a threshold of at least 50 SNP markers for a positive CNA to be ascertained. In the output of HMM copy number analysis, 1,310 regions with a copy

Table 1. Significant Copy Number (CN) Alteration Regions (Region $P < 0.001$ in segmentation) in MPNSTs and PNFs

Patient ID	Tumor	Paired analysis number of CN gain	Paired analysis number of CN loss	Unpaired analysis number of CN gain	Unpaired analysis number of CN loss
M1	MPNST		1	8	18
M2	MPNST	37	61	35	65
M3	MPNST	64	76	61	75
M4	MPNST			9	23
M5	MPNST	11	13	15	32
M7	MPNST	68	102	50	63
M8	MPNST	131	129	68	107
M9	MPNST	61	23	39	34
M10	MPNST	1	1	7	18
M11	MPNST			7	25
M12	MPNST			9	13
M13	MPNST			9	9
M14	MPNST	10	16	19	42
MX	MPNST	44	146	41	121
P1	PNF	16	1	23	28
P2	PNF	1		18	30
P3	PNF	6		20	24
P4	PNF	1	1	27	33
PX	PNF			26	38

Table 2. Multiple Overlapping Regions with LOH in MPNST DNA Not Found in Benign Tumor DNA

Categories of LOH or genes	LOH	LOH genes
Overall	7,643	39,847
Benign tumors	78	117
Overlap in benign tumors	0	0
Malignant tumors	7,565	39,730
Overlap in two MPNSTs	8,159	15,122
Overlap in five MPNSTs	445	543
Overlap in six MPNSTs	40	529

number of 2 and a *P* value of ∼1.00 were then subsequently merged with the 7,643 LOH regions to identify overlaps. In total, 9,188 overlapping regions of potential CNN–LOH were identified. Following filtration of these 9,188 regions with a 0% heterozygosity call rate and the requirement for a minimum of 50 SNP markers in each region, the number of CNN–LOH regions was reduced to 512 because a majority of the LOH regions had fewer than 50 SNP markers. By further applying the criterion that each region must either occur in at least two unrelated patients, the CNN–LOH regions were reduced to 71 (CNN–LOH regions detected in two to four patients). The 71 identified regions were variously located on chromosomes 1, 4, 5, 9, 16, 17, 18, and X. The CNN allele imbalance approach was also applied in the analysis. Paired copy number analysis was performed using segmentation on the 19 pairs of samples. With the segmentation algorithms, at least 50 SNP markers, a *P* value of 0.001, and a signal-to-noise ratio of 0.5 set as threshold; 599 regions were found to have a *P* value of ∼1.00 or were unchanged in copy number in the segmentation. In the SCNA analysis, 3,768 regions are detected for SCNA imbalance. By overlapping the 599 CNVs from the total copy number analysis with the 3,768 regions from the SCNA analysis, we identified 578 regions of CNN imbalance with recurrence in two or more patients. Most of the 578 regions were identified in five or more patients.

Identification of Potential Genes Associated with MPNST Development

Biological pathway analysis

A variety of genes were contained within those CNAs that were found exclusively in MPNSTs. These included *ITGB8* (7p15.3), *PDGFA* and Ras-related C3 botulinum toxin substrate 1 (*RAC1*) (7p22), *PDGFRB* (5q31-q32), and matrix metallopeptidase 12 (*MMP12*) (11q22.3). A biological pathway analysis was performed on the 1,521 genes that were associated with MPNST-specific CNAs, as identified by the MetaCore database (http://www.genego.com/metacore.php). MetaCore is an integrated software suite designed for the pathway analysis of array experimental data. The specific pathways deemed to be potentially involved are listed in Table 3 and Supp. Table S5, together with the map name, cell process, and hypergeometric *P* value found in the present study and in the entire pathway.

The details of these individual pathways are given in Supp. Figure S3. The main conclusion from this analysis was that the genomic aberrations present exclusively in MPNST DNA comprise both specific CNAs and widespread LOH, whereas no such genomic changes were evident in DNA from any benign PNF tumor.

A similar biological pathway assessment was undertaken on the 543 genes shown to be consistently affected by informative LOH changes in DNA from at least five MPNSTs from unrelated patients. The top 10 pathways identified are listed in Table 3. Many of these pathways are involved with cell growth, cell adhesion, signal transduction, and the immune response, and are therefore broadly representative of the systems frequently found to be involved in tumorigenesis and metastasis. This study has therefore identified a number of genes with potential links to the process of NF1 tumorigenesis, including genes directly involved in cytoskeletal remodeling and cell adhesion. For example, at least seven members of the Rho–GTPase gene family known to mediate cytoskeletal remodeling (*ACTB*, *ACTG1*, *LIMK1*, *PRKCA*, *PTK2*, *RAC1*, and *ROCK2*) (Supp. Fig. S3) were found to be associated with recurrent copy number gains in MPNST DNA. In addition, both *ACTB* and *ACTG1* are cytoplasmic actin genes. Hence, their increased expression (as a likely consequence of gene duplication) may influence either the motility or the invasive properties of affected tumor cells (Table 3 and Supp. Table S5).

The relationship between copy number changes and gene expression was assessed by qPCR and a correlation was noted for the majority (∼90%) of the genes analyzed (Supp. Fig. S4a and b). All CNAs identified in this analysis were confirmed by real-time (RT) qPCR and at least seven genes in the Rho–GTPase pathway were found to be amplified (Supp. Fig. S4b). Four of these seven Rho–GTPase pathway genes have been shown to be involved in some of the features of NF1 tumorigenesis, namely, wound healing, cellular

Table 3. The Top 10 Affected Biological Pathways Predicted to be Involved in NF1 Tumorigenesis as Deduced from the 543 Genes Found to Display Consistent LOH in Five MPNSTs Derived from NF1 Patients

Map	Cell process	*P* Value	Objects from LOH gene list	Total objects
Cell adhesion_ECM remodeling	Cell adhesion	0.0064	6	51
Apoptosis and survival_Lymphotoxin-beta receptor signaling	Immune response, apoptosis	0.0109	5	41
Immune response_Role of TLRs 3 and 4 in cell antiviral response: TICAM1-specific signaling pathways	Immune response	0.0207	3	18
Immune response _Oncostatin M signaling via JAK-Stat in mouse cells	Cytokine and chemokine mediated signaling pathway, immune response	0.0207	3	18
wtCFTR and delta508 traffic / Clathrin coated vesicles formation (norm and CF)		0.0240	3	19
Immune response _Oncostatin M signaling via JAK-Stat in human cells	Cytokine and chemokine mediated signaling pathway, immune response	0.0275	3	20
Immune response _Oncostatin M signaling via MAPK in mouse cells	Cytokine and chemokine mediated signaling pathway, immune response	0.0280	4	35
Immune response_Oncostatin M signaling via MAPK in human cells	Cytokine and chemokine mediated signaling pathway, immune response	0.0336	4	37
Immune response _Histamine H1 receptor signaling in immune response	Immune response, G-protein coupled receptor protein signaling pathway	0.0431	4	40

adhesion, migration, and invasion in this study. Alteration of the Rho–GTPase-encoding *RAC1* gene has been identified in multiple solid cancer types including testicular, gastric, and breast cancer in addition to chronic myelogenous leukemia and primary human schwannoma cells [Harnois et al., 2003; Kaempchen et al., 2003].

Immunohistochemistry

For all four proteins, RAC1, ROCK2, LIMK1, and PTK2, greater intensity of cytoplasmic staining was observed in MPNSTs versus benign neurofibromas, both cutaneous and plexiform (data not shown). This finding is consistent with the results obtained by array and qPCR analysis. In neurofibromas, the vast majority of nuclei, blood vessels, and mast cells were stained, whereas in MPNST few nuclei were stained. The pattern of staining was similar for all four proteins in both the tumor types (data not shown) [Bartley & Ross, 2002].

Exploring the involvement of RAC1, ROCK2, PTK2, and LIMK1 in wound healing and cell adhesion, migration, and invasion

RAC1, *ROCK2*, *PTK2*, and *LIMK1* were selected for further functional studies not only because they are key members of the Rho–GTPase pathway and have been implicated in many cancers [Malliri and Collard, 2003] but also because MPNST-specific copy number gains were observed for these genes. In addition, shRNAs for these four genes have been fully validated. All three MPNST cell lines ST8814, 507.1, and T529 used in this study exhibited copy number gains and overexpression of these genes (data not shown).

Wound healing is an intricate process in which the skin (or another organ–tissue) repairs itself after injury. In order to explore the potential role of the overexpression of *RAC1, ROCK2*, *PTK2*, and *LIMK1* on wound healing, cells transfected with *RAC1, ROCK2, PTK2*, and *LIMK1* knockdowns and scrambled control shRNA were seeded onto laminin and wounded with a pipette tip. Between 0 and 12 hr after wounding, the cells migrated across the wound. Wound healing was reduced in *RAC1*, *ROCK2*, *PTK2*, and *LIMK1* knockdown cells by comparison with control scrambled shRNA (Fig. 3a; data for *PTK2* and *LIMK1* provided in Supp. Fig. S5a and b). Owing to the kinetics of wound healing, healing was deemed to be complete when no gap was observed in all shRNA cell lines by 24 hr, although healing occurred earlier (12–16 hr) in the control cell line than in the *RAC1*, *ROCK2*, *PTK2*, and *LIMK1* knockdown cell lines (16–24 hr). The above experiment was repeated on a further three cell lines (ST8814, 507.1, and T529). All experiments were repeated a minimum of three times and the results generated from each of the three experiments were in concordance. MPNST cell doubling time is approximately 20.44 hr (ST8814) [Vahidnia et al. 2007]. Wound healing is unlikely to have been affected by cell proliferation as wound healing was observed by 12 hr in the scrambled control cell line.

Cell adhesion is a complex mechanism involved in a variety of processes including cell migration and invasion, embryogenesis, wound healing, and tissue remodeling. In order to explore the potential role of the overexpression of *RAC1*, *ROCK2*, *PTK2*, and *LIMK1* on cell adhesion, cells were transfected with *RAC1* and *ROCK2* knockdown and control shRNAs on both laminin and fibronectin, and *PTK2* and *LIMK1* with control shRNA on laminin. Adhesion was significantly increased in cell lines containing *RAC1*, *ROCK2*, *PTK2*, and *LIMK1* knockdowns ($P = 0.02$, $P = 0.05$, $P = 0.001$, and $P = 0.002$, respectively) by comparison with cell lines transfected with the scrambled control shRNA (Fig. 3b) (data for *PTK2* and *LIMK1* in Supp. Fig. S4a and b). *RAC1* knockdown resulted in greater cell adhesion than *ROCK2* knockdown, and *LIMK1* knockdown resulted in greater cell adhesion than *PTK2* knockdown. However, these differences were not statistically significant, $P = 0.07$ and $P = 0.12$, respectively. Adhesion on fibronectin appeared to be more efficient than that on laminin in cell lines harboring both *RAC1* and *ROCK2* knockdowns, but again this difference was not statistically significant ($P = 0.20$).

Cell migration is a highly integrated, multistep process that plays an important role in the progression of cancer. In order to explore the potential role of the overexpression of *RAC1*, *ROCK2*, *PTK2*, and *LIMK1* on cell migration, the migration of cells transfected with *RAC1*, *ROCK2*, *PTK2*, and *LIMK1* and control shRNA was assessed by seeding the cells onto polycarbonate membranes [de Pril et al., 2009]. Cell migration was significantly reduced in *RAC1*, *ROCK2*, *PTK2*, and *LIMK1* knockdown cell lines in comparison with cells transfected with a scrambled vector ($P = 0.05$, $P = 0.03$, $P = 0.025$, and $P = 0.027$, respectively) (Fig. 3c). The reduction in migration was similar in cells that were transfected with *RAC1*, *ROCK2*, *PTK2*, and *LIMK1* (Fig. 3C) (data for *PTK2* and *LIMK1* in Supp. Fig. S5). Approximately 40% reduction in cell migration was observed in 80% knockdowns of *RAC1*, *ROCK2*, *PTK2*, and *LIMK1* and approximately 25% reduction in 50% knockdowns of *RAC1*, *ROCK2*, *PTK2*, and *LIMK1*. Results were representative of all cell lines and replicates (ST8814, 507.1, and T529).

Tumor cell invasion into the basement membrane is an important step in the multistep process of tumor metastasis. The potential role of the overexpression of *RAC1* and *ROCK2* on the invasive properties of cells transfected with *RAC1* and *ROCK2* knockdowns and control shRNAs was assessed by seeding cells onto matrigel basement membrane on polycarbonate membranes. A significant reduction in the invasive potential of cell lines transfected with both *RAC1* and *ROCK2* knockdown shRNA was observed by comparison with the scrambled control ($P = 0.05$ for both) (Fig. 3d and e) This analysis was not performed for *PTK2* and *LIMK1*. *RAC1* and *ROCK2* knockdowns elicited a similar reduction in invasive potential; an approximately 45% reduction in cell invasion was observed with both *RAC1* and *ROCK2* 80% knockdown clones as compared with the scrambled control-transfected cell line. Similarly, a 25% reduction in invasion was seen in both genes carrying 50% knockdown clones. All experiments were repeated and the results were comparable in all three cell lines (ST8814, 507.1, and T529) tested. In summary, both *RAC1* and *ROCK2* knockdown resulted in a reduction in wound healing, cell migration, and invasiveness and an increase in cell adhesion.

Validation of specific gene knockdown using shRNA clones was completed by western blot analysis followed by densitometry using Image J software (http://rsbweb.nih.gov/ij/) (Fig. 3f).

Discussion

Neurofibromin, the *NF1* gene product, is a tumor suppressor protein whose main function is to downregulate Ras activity in the cell. The mutational inactivation of the *NF1* gene, leading to loss of functional neurofibromin, therefore, results in the constitutive activation of cellular Ras, as well as the associated RAS/RAF/MAPK signaling pathway, leading to increased cell growth and proliferation and an increased likelihood of tumorigenesis [Guha et al., 2006; Upadhyaya, 2010]. The majority of the somatic *NF1* mutations identifiable in both benign and malignant NF1-associated tumors serve to inactivate the normal *NF1* allele [Knudson, 1971]. However, the presence of biallelic *NF1* inactivation in both benign and malignant tumors indicates that constitutive Ras activation cannot fully explain the malignant transformation of a benign PNF to an MPNST and that additional genetic (or epigenetic) alterations are required to

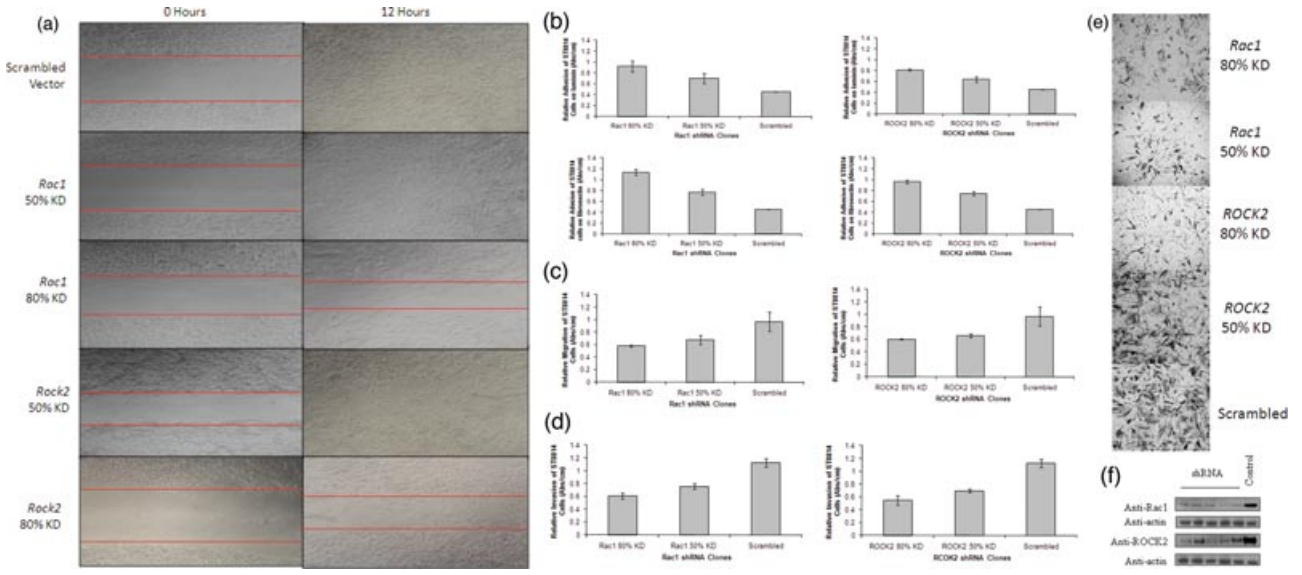

Figure 3. (A) Wound healing assay on MPNST cell line ST8814. Cells were seeded on laminin, syncronized in 1% FBS for 24 hr and wounded with a pipette tip. Wounds were followed up for 24 hr. Reduction in the rate of wound healing can be seen in the cell lines carrying *RAC1* and *ROCK2* knockdowns. Cells were imaged on a microscope at ×10 magnification (Leica). (B) Adhesion assay on MPNST cell line ST8814. (i) ST8814 cells transfected with *RAC1* shRNA seeded on laminin, (ii) *ROCK2* shRNA-transfected cells seeded on laminin, (iii) cells transfected with *RAC1* shRNA on fibronectin, and (iv) *ROCK2* shRNA-transfected ST8814 cells seeded on fibronectin. Adhesion was significantly increased in samples containing *RAC1* and *ROCK2* knockdowns in comparison with a cell line transfected with the scrambled control shRNA ($P = 0.02$) and ($P = 0.05$), respectively. The *RAC1* knockdown results in more cell adhesion than the *ROCK2* knockdown but this difference was not significant ($P = 0.07$). Adhesion on fibronectin was more efficient than that on laminin in cell lines carrying both *RAC1* and *ROCK2* knockdown, but again this observed difference was not significant ($P = 0.2$). All results were a readout of the absorbance of crystal violet (5 mg/ml) eluted with 1% SDS at 550 nm on a Genova MK3 Lifescience Analyser (Jenway). (C) Migration assay on ST8814 cell lines. (i) Migration of ST8814 cells transfected with *RAC1* shRNA, (ii) migration of ST8814 cells transfected with *ROCK2* shRNA. Migration of ST8814 cells was significantly reduced in cell lines carrying *Rac1* and *ROCK2* knockdowns in comparison with ST8814 cells transfected with a scrambled vector ($P = 0.05$ and $P = 0.03$, respectively). The reduction in migration was similar in cells transfected with both *RAC1* and *ROCK2*. 1.34×10 fewer cells migrated through the membrane in the cell line with the *RAC1* 80% knockdown and 1.3×10^6 fewer cells migrated in the *ROCK2* 80% knockdown cell line as compared with the scrambled control. All results were a readout of the absorbance of crystal violet (5 mg/ml) eluted with 1% SDS at 550 nm on a Genova MK3 Lifescience Analyser (Jenway). (D) Invasion assay on ST8814 cell lines. (i) Invasion of ST8814 cells transfected with *RAC1* shRNA. (ii) Invasion of ST8814 cells transfected with *ROCK2* shRNA. The invasion activity of ST8814 cell lines was significantly reduced in those cell lines with both *RAC1* and *ROCK2* knockdown as compared with the scrambled control ($P = 0.05$ for both). *RAC1* and *ROCK2* knockdowns elicited similar reductions in invasive potential of the ST8814 cells. 1.85×10^6 fewer cells invaded the matrigel and membrane in the cell line with the RAC1 80% knockdown and 1.8×10^6 in the *ROCK2* 80% knockdown as compared with the control scrambled cell line. All results were a readout of the absorbance of crystal violet (5 mg/ml) eluted with 1% SDS at 550 nm on a Genova MK3 Lifescience Analyser (Jenway). (E) Invasion assay on ST8814 cells transfected with *RAC1*, *ROCK2*, and scrambled control shRNA. Cells were stained with crystal violet (5 mg/ml) and images were taken at ×10 magnification (Leica). *RAC1* and *ROCK2* knockdown elicited a reduction in the invasive potential of ST8814 cell lines as evidenced by the lack of *RAC1* and *ROCK2* shRNA-transfected cells on the underside of the membrane following 3 days incubation. All experiments were repeated a minimum of three times. Results were similar for all three MPNST cell lines studied (ST8814, 507.1, and T529). All statistical analysis was completed with SPSS v16 using independent samples *t*-test. (F) Western blot assay of cell lines transacted with 5 *RAC1* and *ROCK2* shRNA clones in addition to one cell line transfected with a scrambled control. β-actin control blots were completed to ensure expression was unaffected in genes not targeted by the shRNA.

drive such transformation. In order to better understand the basis of tumorigenesis in NF1, the detailed characterization of all malignant tumor-associated genetic/genomic defects will be required. However, the somatic inactivation of cancer-associated genes may involve many different mutational mechanisms, from point mutations to large genomic rearrangements and even epigenetic changes [Bignell et al., 2010; Stratton et al., 2009; Kops et al., 2005; Rajagopalan et al., 2004. In NF1 tumors, somatic microlesions as well as LOH and CNAs are likely to play a key role in malignant transformation (reviewed by Upadhyaya, 2011)].

Both LOH analysis and/or direct somatic mutation screening at the *NF1* locus have been reported for many NF1-associated tumors (both benign and malignant), including cutaneous and PNFs, MPNSTs, pheochromocytomas, myeloid leukemias, gastrointestinal tumors, glomus tumors, and bone tumors [Serra et al., 2000; Upadhyaya et al., 2004, Garcia-Linares et al., 2011; Bausch et al., 2007; Side et al., 1997; Stewart et al., 2007, 2008; Maertens et al., 2006; Brems et al., 2009b, Stevenson et al., 2006]. Such genetic analyses of MPNSTs have clearly shown that biallelic *NF1* gene inactivation only occurs in the component Schwann cells or glial cells of these NF1-related tumors. What is still puzzling, however, is why only 10–15% of PNFs undergo malignant transformation to MPNSTs even though both cutaneous and PNFs have essentially the same cellular constitution. Alterations of other regions of the genome have also been detected in several NF1-related tumors including MPNSTs; these are known to involve the *TP53*, *CDKN2A*, and *RB1* genes [Brems et al., 2009a; Cichowski and Jacks, 2001]. In contrast to the specific chromosomal translocations found in many synovial (and other types of) sarcoma, no consistently specific pathogenic chromosomal aberrations are known to be associated with MPNSTs, although a number of small recurring chromosomal alterations have been reported. Indeed, several cytogenetic studies have noted that MPNSTs possess complex karyotypes characterized by a wide spectrum of chromosomal aberrations including translocations and duplications as well as numerical gains and losses [Bridge et al., 2004; Fang et al., 2009]. Frequent deletions of the 9p21 region

containing the *CDKN2A* (p16) gene have been reported in several NF1–MPNSTs [Cairns et al., 1995; Frahm et al., 2004; Nielsen et al., 1999; Perrone et al., 2003; Sabah et al., 2006]. At least two other regions on chromosome 17, in addition to that containing the *NF1* gene at 17q11.2, appear to be involved in NF1 tumorigenesis, with gains at 17q21-q22 potentially accounting for the reported upregulation of the *TOP2A* gene from this chromosomal region in patients harboring MPNSTs and who have a poor disease outcome [Skotheim et al., 2003]. Loss of the 17p13 region, encompassing the *TP53* gene, has been noted not only in NF1–MPNSTs [Legius et al., 1994; Lothe et al., 2001] but also in soft sarcomas and other cancers [Borrás et al., 2011; Latres et al., 1994]. In similar vein, aberrant expression of proteins of the Rb pathway has been associated with soft-tissue sarcomas including MPNSTs [Mawrin et al, 2002].

The identification of tumor-specific genomic copy number changes in a range of different cancers [Weir et al., 2004; Suzuki et al., 2008; Chen and Chen, 2008; Dear, 2009; Kuiper et al., 2010; Park et al., 2010; Barretina et al., 2010] has led to the increased use of SNP and CNV/CNA microarray platforms to screen tumor DNAs. Previous studies aimed at identifying the global genetic changes present in benign and malignant NF1 tumors have variously applied gene expression profiling and RT-PCR analysis to RNA from both benign and malignant tumors in order to identify specific gene expression signatures associated with malignancy. Significant alterations in the expression of many genes have been reported in MPNSTs, including the *TP53*, *RB1*, *CDKN2A* (p16INK4A and p14/ARF), *CDKN1B* (p27/KIP1), *TWIST1*, *SOX9*, *SOX10*, *TNC*, *TRIO*, *NKD2*, *IRX2*, tenascin C and tenascin XB, and *EGFR* loci [Lévy et al., 2004; Miller et al., 2006, 2009; Lévy et al., 2007 reviewed by Upadhyaya, 2011]. Although CNAs have been reported in many primary tumors, few such studies of NF1 tumors have so far been undertaken. Initially, we constructed an exon-based cancer gene microarray that specifically targeted 57 different genes whose expression had previously been reported to be significantly altered in MPNSTs [Mantripragada et al., 2008]. Subsequently, a 32K BAC array was used to analyze DNA from both benign neurofibromas and MPNSTs, thereby providing a genome-wide analysis of large [up to 150 kb] copy number changes potentially associated with progression to malignancy [Mantripragada et al., 2009] with an average resolution of 100 kb. However, the relatively low resolution of this array platform meant that many smaller (≤100 kb) genomic variants were unlikely to be identified, leading us here to repeat such a genome-wide analysis using the newly available Affymetrix Genome-wide SNP 6.0 platform, which permits the simultaneous high-resolution analysis of both CNA and LOH.

In a number of such microarray CNA studies, significant variability using different array platforms has been obtained when similar tumor types are analyzed [Dear, 2009]. Whether such variability arises from the different microarray platforms (BAC, PAC, SNPs, and oligonucleotides) used, or from the variable size, number, and genomic distribution of the probes in the microarray, or whether it relates to the inherent genetic heterogeneity of the tumors themselves, is often difficult to determine. We have found, however, that the Affymetrix SNP 6.0 platform provides both increased resolution (with an average interprobe distance of only 700 bp) and significantly greater genome-wide coverage (with 0.9×10^6 SNP probes and 0.95×10^6 CNV probes) by comparison with the older 32K BAC array [Kresse et al., 2008; Mantripragada et al., 2008, 2009].

A total of at least 17 different studies have now attempted to assess the chromosomal and genomic copy number changes associated with NF1-related tumors (see Table 4). Taken together, these studies indicate that genes involved in cell cycle regulation, cell growth, cell differentiation, and motility are specifically altered in terms of their copy number in MPNSTs. The present study has not only served to confirm these initial findings but also, courtesy of its higher resolution, identified additional genes that appear to be involved in MPNST development. For example, across chromosome 17, we find that several regions exhibit recurring copy number changes in MPNSTs; apart from the obvious 17q11.2 region containing the *NF1* gene, two quite distinct regions at 17q22 and 17q24-q25 were also found to be frequently amplified in MPNSTs, whereas one region at 17p13 was consistently deleted in MPNSTs. The 17q24-25 region, which contains the *BIRC5* gene, a gene previously reported to be amplified in MPNSTs [Storlazzi et al., 2006] and consistently upregulated in many other tumors [Kanwar et al., 2010], was found to be amplified in four MPNSTs. Survivin, the *BIRC5* gene product, is a central inhibitory protein of apoptosis that also regulates mitosis. The 17q22 region, amplified in two MPNSTs in our study, contains the *TOP2A* gene known to play a role in cell proliferation [Skotheim et al., 2003]. The 17p13 region, which contains the *TP53* gene, was found to be deleted in four MPNSTs but not in any of the benign tumors. Our CNA study also identified consistent amplification of the entire 5p region, reminiscent of findings from a previous CNA analysis of soft-tissue sarcomas [Adamowicz et al., 2006]. This latter study, which also analyzed 10 NF1-associated MPNSTs, found that most of the 5p13-p15.3 region was amplified in several different MPNSTs. Several of the 5p13-p15.3 region genes, including *TRIO*, *IRX2*, and *NKD2*, were also found to exhibit increased expression specifically in MPNSTs [Adamowicz et al., 2006]. *TRIO* is a member of the large family of guanine nucleotide-exchange factors that activate Rho–GTPases, specifically the RAC1 and RhoA Rho family GTPases, by accelerating GDP/GTP exchanges. *TRIO* has been implicated in the control of cytoskeleton organization, transcriptional regulation, cell cycle progression, apoptosis, vesicle trafficking, and cell–cell adhesion, whereas significant *TRIO* gene amplification has been previously associated with both rapid tumor cell proliferation and increased invasive tumor growth in bladder cancer [Zheng et al., 2004].

Our earlier study found that the hepatocyte growth factor (*HGF*) gene, the cellular HGF receptor (*MET*) gene, and the platelet-derived growth factor receptor A (*PDGFRA*) gene were concomitantly amplified (despite their being located on different chromosomes) in a number of MPNSTs but not in PNFs or cutaneous neurofibromas [Mantripragada et al., 2008]. The HGF–PDGFRA–p70S6K pathway is known to play an essential role in tumor angiogenesis, and rapamycin treatment could therefore be considered as a means to limit tumor growth by inhibiting p70S6K. In the present study, *MET* displayed a copy number of 2.8–3.0 in M3, M5, and MX, whereas *PDGFRA* displayed a copy number of 3–4 in MX (but only 1.2–1.5 in M3 and M7).

Our previous 32K BAC array-based analysis [Mantripragada et al., 2009] of MPNST DNA revealed that genomic gains (62%) were much more frequent than genomic losses (38%) in these malignant tumors. A number of genes were also consistently amplified in MPNSTs; indeed, the *NEDL1*, *AP3B1*, and *CUL1* genes located at 7q, 5q14, and 7q36 were amplified in some 60% of tumors [Mantripragada et al., 2009]. The most frequently deleted region, at 9p21, which encompasses the *CDKN2A*, *CDKN2B*, and *MTAP* genes, was, however, only deleted in some 30% of tumors. Several of the abovementioned six genes have also been implicated in a number of other cancers [Goh et al., 2011; Mizuarai et al., 2011] and they may, therefore, prove to have potential diagnostic, prognostic, and even therapeutic relevance in the context of NF1 tumorigenesis.

The results of the Affymetrix SNP 6.0 analysis described here extended our previous findings [reviewed by Upadhyaya, 2011] based on different sets of benign and malignant tumors with

Table 4. Reported CNAs Identified in Different NF1-Associated Tumors

References	Tumors studied	Analytical methods used	Gene or chromosomal changes	
			Gains	Losses
Lothe et al. (1995, 1996)	Neurofibromas (15) MPNSTs (9)	17q LOH study FISH analysis	–	17q allelic imbalance 4/6 NF1-associated MPNSTs
Lothe et al. (1996)	MPNSTs (7)	Chromosome CGH	Increased 17q24-ter copy number in 5 of 7 tumors	Loss of 13q14-q21 in 6/10 MPNSTs
Kourea et al. (1999)	MPNSTs (11) Primary tumors (8) Recurrent tumors (3)	*INK4A* cDNA probe on Southern blot	–	*INK4A* deletions in ?? MPNSTs
Nielsen et al. (1999)	MPNSTs (6)	Multiplex PCR	–	Homozygous *CDKN2A* deletions in 3 MPNSTs
Schmidt et al. (2000)	MPNSTs (14)	Chromosome CGH	Gains on Chr 7; 8q; 15q; 17q	–
Skotheim et al. (2003)	MPNSTs (14) MPNSTs (16) MPNSTs (44)	Combined analyses 1) Chr:17-specific cDNA microarray 2) FISH analysis 3) Tissue microarray	*TOP2A* overexpressed in most MPNSTs	–
Levy et al. (2004)	MPNSTs (9) PNF (16) Dermal NF (10)	Real-time quantitative PCR on tumor RNA	*MK167, BIRC5, MMP13, MMP9, TERT, TERC, TOP2A, SPP2, FOXM1, FOXA2, HNF3B, HMMR, CXCL5, OSF2, CCNE2, EPHA7* and *TP73* only upregulated in MPNST	*ITGB4, CMA1, LICA1, DHH, S100B, ERBB3, RASSF2, TPSB* and *SOX10* all downregulated only in MPNSTs
Adamowicz et al. (2006)	Soft-tissue sarcomas (34) included MPNSTs (10)	Chr:5p BAC microarray	*TRIO, IRX2,* and *NKD2* all located at 5p15.3 are amplified	–
Miller et al. (2006)	Primary MPNSTs (44) MPNST cell lines (8) Normal Schwann cells (7)	Gene expression profiling (Affymetrix chip)	*EDGRE, SOX9, TWIST1*	*SOX10, CNP, PMP2*
Storlazzi et al. (2006)	MPNSTs (28) Primary tumors (25) Recurrent tumors (2) Metastatic tumor (1)	Interpase FISH analysis of 17q with BAC probes	*ERBB2* and *TOP2A* in 17q12>17q25 amplicon that also contains *BIRC5*	–
Kresse et al. (2008)	High-grade MPNSTs (7)	Array CGH	*LOXL2, TOP2A, ETV4,* and *BIRC5*	–
Tabone-Eghanger et al. (2008)	MPNSTs (42)	FISH	*EGFR*	–
Mantripragada et al. (2008)	MPNSTs (35) PNFs (16) Derm NFs (8)	Targeted gene array	*ITGB4, PDGFRA, MET, HGF* and *PP73*	*NF1, HMMR, MMP13, INK4A* and *CDKN2B*
Perrone et al. (2009)	Sporadic MPNST (11) NF1 MPNST (16)	COMBINED ANALYSES 1) FISH 2) Gene activation 3) Mutational analysis	*PDGFRA* and *PDGFRB EGFR* copy number	–
Mantripragada et al. (2009)	MPNSTs (24)	32K BAC genomic array	*NEDL1, AP3B1,* and *CUL1*	*CFKN2A* and *CDKN2B*
Miller et al. (2009)	MPNST cell lines (13) Neurofibromal Schwann cells (22) Primary MPNSTs (6)	Gene expression profiling (Affymetrix chip) Affymetrix	*SOX9, TWIST1*	–
Yu et al. (2011)	Primary MPNSTs (125)	Affymetrix Genome-Wide 500K SNP	*CDK4, FOXM1, SOX5, NOL1, MLF2, FKBP4, TSPAN31*	*ERBB2, MYC, TP53*

recurrent MPNST-specific amplified CNAs being found at 1q24, 1q34, 17q23.2, and 8p23. These copy number changes have already been noted to affect a variety of different genes including *ITGB4*, *BIRC5*, *MET*, *ETV4*, *TWIST1*, *TRIO*, *NKD2*, *IRX1*, *IRX2*, *IRX4*, *EGFR*, *SOX9*, *HOXB5-9*, *TOP2A*, *MMP13*, *TP53*, *CDKN2A*, *RB1*, *TNC*, *HMM*, *CDK4*, and *FOXM1* (Table 4). The use of the Affymetrix SNP 6.0 Array in this study led to the identification of several additional genes that were consistently amplified in MPNSTs, including the *ITGB8*, *PDGFA*, and *RAC1* genes (all at 7p21.1-p22) and the *PDGFRL* gene (8p22-p21.3), and the *MMP12* gene (11q22.3), which was deleted in MPNSTs.

The amplification in MPNSTs of two related integrin genes, *ITGB4* at 17q25 and *ITGB8* at 7p21.1-p22, is intriguing because integrin signaling regulates the metastatic cancer phenotype [Guo, 2004], mainly through synergistic interactions with several critical signaling pathways, including the Ras/Raf/MAPK pathway, the Rho-effector pathway, and the epidermal growth factor receptor pathway [Schubbert et al., 2004]. The *RAC1* gene is a member of the Rac subfamily of the large family of Rho–GTPases directly involved in cell signaling and the regulation of cell growth, cell–cell adhesion, cytoskeletal reorganization, and the activation of protein kinases. RAC1 protein interacts with the T-cell lymphoma invasion and metastasis-inducing protein 1 and both are upregulated in nasopharyngeal carcinoma [Gao et al., 2001; Wu et al., 2007; Qi et al., 2009; Worthylake et al., 2000]. The *MMP12* gene is one of several MMP genes located at 11q22.3. As with most other MMP proteins, activated MMP12 degrades soluble and insoluble elastin, and is directly involved in extracellular matrix protein degradation [Shapiro, 1998, 1999]. MMP12 has been reported to be involved in glioma cell invasion in the brain, apparently through its direct interactions with tenascin C [Erickson and Bourdon, 1989]. Changes in *MMP12* gene expression might therefore be expected to accompany increased invasiveness of central nervous system (CNS) tumors. As the PDGF signaling system is upregulated in many cancers, the finding of coamplification of the *PDGFA* and *PDGFRL* genes in four MPNSTs in the present study may well be functionally significant. A previous investigation of the PDGF pathway in MPNSTs also noted increased expression of *PDGFRA* and *PDGFRB*, as well as the *EGFR* gene where increased gene expression and protein phosphorylation was found to correlate with gains in *EGFR* copy number [Perrone et al.,

2007]. A more recent study also reported increased *EGFR* expression and *PDGFRA* amplification in MPNSTs and noted that both features were associated with a poor prognosis [Tabone-Eglinger et al., 2008]. Once activated, EGFR and PDGFR stimulate tyrosine kinase activity and intracellular pathways that control proliferation and differentiation.

The present study identified a much larger number of deleted genomic regions in MPNSTs than the two previous studies [Kresse et al., 2008; Mantripragada et al., 2009]. However, we failed to identify any relationship between the grade of MPNSTs (Supp. Table S1) and the CNA profile. Furthermore, the copy number profiles generated from the individual MPNSTs appear to identify two distinct subgroups of malignant tumors: those with a major CNA profile (tumors M2, M3, M6, M7, M8, and M15) and those with a minor CNA profile (tumors M4, M10, M11, M12, and M13) comparable with the copy number profiles obtained from benign PNFs. It is perhaps difficult to reconcile these data pertaining to inter-MPNST heterogeneity, especially as several of the MPNSTs in both subgroups were classified as high-grade tumors. Similarly, the finding of a high-CNA profile associated with a benign PNF (P116) derived from a sporadic NF1 patient is puzzling, although one explanation could be that this PNF was in transition toward MPNST development. This disparity in CNA profiles between apparently high-grade MPNSTs may also be a consequence of the considerable somatic genetic heterogeneity associated with these malignant tumors [reviewed by Upadhyaya, 2011] and further highlights the significant diagnostic and therapeutic challenges posed by these histologically complex and genetically highly heterogeneous tumors [Stasik & Tawfik, 2006; Spurlock et al., 2010].

Loss-of-heterozygosity and CNAs are only two of the many genetic mechanisms potentially involved in NF1 tumorigenesis. Hence, MPNSTs lacking a significant number of CNAs may harbor microlesions and/or aberrant methylation of gene promoter regions. However, the significant degree of LOH found in most MPNSTs, LOH that is essentially absent from benign neurofibromas, confirms our previous finding that many NF1-associated MPNSTs harbor large somatic *NF1* deletions [Upadhyaya et al., 2008; Botillo et al., 2009]. Furthermore, CNN–LOH analysis indicated that CNN–LOH is less common than LOH (allelic imbalance) in the development of MPNSTs and this concurs with our earlier finding.

This study is the first to assess both LOH and CNA within the same panel of MPNST and PNF tumors. This approach has yielded new insights into the biological pathways involved in the malignant transformation of PNFs in NF1. This study has also identified a number of candidate genes that may be involved in MPNST development. Further studies of these genes should now be performed with a larger set of tumor samples, both to confirm the copy number changes and to seek additional types of tumor-associated mutation within these genes.

It is unclear what would be the net effect of the observed CNAs on cellular properties and how this would impact upon tumorigenesis. A better understanding of how such CNAs influence the expression of the genes they encompass is required in order to assess their possible role in tumorigenesis. Such studies are ongoing, one of which directly assessed the impact that SNPs and CNVs have on gene expression, finding that less than 20% of gene expression variability was directly attributable to CNVs of ≥40 kb in size [Henrichsen et al., 2009a, 2009b]. In addition, at least half of the genes whose expression was directly influenced by a CNV were actually located outside the relevant CNV [Henrichsen et al., 2009a, 2009b], an indication that many CNVs affect gene regulatory sequences located at some distance from the target gene. A genetic pathway represents a set of interactions occurring within and between a group of genes that are dependent upon each other's individual functions in order to make the aggregate function of the network available to the cell. Gene pathways are composed of multiple genes with coordinated functions. Thus, a genetic mutation disrupting the function of one gene in a pathway necessarily breaks the informational connection between genes acting before and after the mutant gene in that pathway. Several new insights into pathways potentially involved in NF1 tumorigenesis were obtained during the course of this study.

The principal requirements for cancer metastasis to occur include tumor cell adhesion, migration, cell invasion, and wound healing. The present study identified CNAs affecting several genes from the Ras-homologous (Rho)–GTPase signaling pathway (*ACTB*, *ACTG1*, *LIMK1*, *PRKCA*, *PTK2*, *RAC1*, *ROCK2*, and *TRIO*) specifically in MPNSTs. The potential involvement of this signaling pathway in tumor development is likely to be important because Rho–GTPases are key regulators of actin reorganization, cell motility, cell–cell and cell–extracellular matrix adhesion, cell cycle progression, gene expression, and apoptosis [Etienne-Manneville and Hall, 2002], processes that are involved in both malignant transformation and metastasis. Many of the copy number gains observed in our study may therefore be directly implicated in the malignant transformation from benign PNF to malignant MPNST through the promotion of cell proliferation, motility, and metastasis and by the specific alteration of the cellular pathways that serve to reorganize the cytoskeletal structures. Functional analysis of MPNST cell lines transfected with shRNAs for *RAC1*, *ROCK2*, *PTK2*, and *LIMK1* indicated that targeted knockdown of at least four of the genes that map to the Rho–GTPase pathway reduces the malignant potential of these cells as evidenced by a significant reduction in wound healing, invasion, and migration and an increase in cell adhesion. On this basis, we propose that it would be worth exploring whether the use of specific inhibitors of individual Rho functions could be used to provide therapeutic benefit in patients with MPNSTs [Fritz & Kaina, 2006]. The use of such an inhibitor in a prostate carcinoma cell line has been shown to inhibit the proliferation, anchorage-dependent growth, and invasiveness of these tumor cells [Gao et al., 2004].

The use of DNA copy number data to explore the process of malignant transformation, as well as to subclassify different tumors, does however have several limitations, the most obvious being that many such tumor-specific CNAs involve multiple genes, many of which are unlikely to be involved in the process of tumorigenesis. Hence, the identification of diagnostically and prognostically applicable genetic markers in tumors is always going to be challenging. Indeed, this is clearly demonstrated in the present study, which revealed that no single gene, or even multiple gene set, was consistently altered in all MPNSTs as compared with PNFs. Other mutational mechanisms will therefore need to be considered in NF1-assocated tumorigenesis, for example, microlesions, increased microsatellite instability, and even epigenetic changes that may influence gene expression either specifically or globally. A major problem with many of the high-resolution analytical technologies recently applied to the study of human tumor genomes is the plethora of somatic mutation data they create. This mass of data then requires careful dissection to identify the very few "driver" mutations from among the many accompanying "passenger" mutations [Stratton et al., 2009]. Unfortunately, this is especially problematic in tumors such as MPNSTs, which exhibit both complex chromosomal abnormalities and significant cellular heterogeneity. A comprehensive study of a large panel of both NF-associated and sporadic MPNSTs, and that integrates copy number change measurements, gene expression analysis, and biologically relevant functional analyses, is clearly warranted. Such studies should follow the example of the comprehensive integrated

genomic analyses that the Cancer Genome Atlas programme have applied to define a range of cancer genomes [Ding et al., 2008; Parsons et al., 2008]. It is intriguing that these and other similar studies consistently identify the presence of inactivating *NF1* gene mutations in many of these tumors including ovarian serous carcinomas [Sangha et al., 2008; Kuo et al., 2009], acute myelogenous leukemia [Mullally and Ebert, 2010], neuroblastoma [Hölzel et al., 2010], lung cancer [Bignell et al., 2010, Ding et al., 2008; Kan et al., 2010], as well as in various other cancers [Kan et al., 2010]. These studies serve to highlight the central role that neurofibromin plays in the function of normal cells and supports the view that the loss of this function is a major cause of tumorigenesis. As somatic gene amplification, paralleled by increased gene expression, is a hallmark of many cancers, the generation of comprehensive maps of copy number variation [Bergamaschi et al., 2006; Lee et al., 2008] and their associated gene expression changes should contribute to a better understanding of the mechanisms through which CNAs promote tumorigenesis. Current challenges involve developing high-resolution methods for determining the association of CNAs with biological function in common cancer.

In summary, we have identified specific genomic changes in MPNSTs as reflected by CNV, LOH, and CNN–LOH analyses. Some 1,521 genes were found to be associated with the specific CNAs in MPNSTs, several of which represent excellent candidates for involvement in tumorigenesis, including novel changes involving *ITGB8*, *PDGFA* and *RAC1* (all 7p21-p22), *PDGFRL* (8p22-p21.3), and *MMP12* (11q22.3). We also report that allelic imbalance in NF1-associated MPNSTs is more prevalent than CNN–LOH, consistent with the view that imbalances of expression are critically important in tumorigenesis. Our other key finding was the involvement of several genes of the Rho–GTPase pathway, which could prove to have a pivotal role in the regulation of processes involved in NF1 tumorigenesis and metastasis. shRNA for *RAC1*, *ROCK2*, *PTK2*, and *LIMK1* were used in adhesion, migration, and wound healing assays and also *RAC1* and *ROCK2* in cell invasion in control and MPNST-derived cell lines. The results of these assays clearly demonstrated that targeted knockdown of such genes is capable of reducing the malignant potential of these cells. Taken together, we have identified several new potential targets for therapeutic intervention during MPNST development.

Acknowledgments

We thank all the patients who have contributed to this study. We are grateful to Dr. Paul Northcote for his comments. We thank Cancer Research UK for their financial support. We are grateful to Dr. Jim Neal for his advice on IHC work and Chris Lovejoy for technical assistance.

Disclosure Statement: The authors declare no conflict of interest.

References

Adamowicz M, Radlwimmer B, Rieker RJ, Mertens D, Schwarzbach M, Schraml P, Benner A, Lichter P, Mechtersheimer G, Joos S. 2006. Frequent amplifications and abundant expression of *TRIO*, *NKD2*, and *IRX2* in soft tissue sarcomas. Genes Chrom Cancer 45:829–838.

Albertson DG. 2006. Gene amplification in cancer. Trends Genet 22:447–455.

Barretina J, Taylor BS, Banerji S, Ramos AH, Lagos-Quintana M, Decarolis PL, Shah K, Socci ND, Weir BA, Ho A, Chiang DY, Reva B, Mermel CH, Getz G, Antipin Y, Beroukhim R, Major JE, Hatton C, Nicoletti R, Hanna M, Sharpe T, Fennell TJ, Cibulskis K, Onofrio RC, Saito T, Shukla N, Lau C, Nelander S, Silver SJ, Sougnez C, Viale A, Winckler W, Maki RG, Garraway LA, Lash A, Greulich H, Root DE, Sellers WR, Schwartz GK, Antonescu CR, Lander ES, Varmus HE, Ladanyi M, Sander C, Meyerson M, Singer S. 2010. Subtype-specific genomic alterations define new targets for soft-tissue sarcoma therapy. Nat Genet 42:715–721.

Bartley AN, Ross DW. 2002. Validation of p53 immunohistochemistry as a prognostic factor in breast cancer in clinical practice. Arch Pathol Lab Med 126:456–458.

Bausch B, Borozdin W, Mautner V, Hoffmann MM, Boehm D, Robledo M, Cascon A, Harenberg T, Schiavi F, Pawlu C, Peczkowska M, Letizia C, Calvieri S, Arnaldi G, Klingenberg-Noftz RD, Reisch N, Fassina A, Brunaud L, Walter MA, Mannelli M, MacGregor G, Palazzo FF, Barontini M, Walz MK, Kremens B, Brabant G, Pfäffle R, Koschker AC, Lohoefner F, Mohaupt M, Gimm O, Jarzab B, McWhinney SR, Opocher G, Januszewicz A, Kohlhase J, Eng C, Neumann HP; European-American Phaeochromocytoma Registry Study Group. 2007. Germline NF1 mutational spectra and loss-of-heterozygosity analyses in patients with pheochromocytoma and neurofibromatosis type 1. J Clin Endocrinol Metab 92:2784–2792.

Bennett E, Thomas NS, Upadhyaya M. 2009. Neurofibromatosis type 1: its association with the Ras/MAPK pathway syndromes. J Pediatr Neurol 7:105–115.

Bergamaschi A, Kim YH, Wang P, Sørlie T, Hernandez-Boussard T, Lonning PE, Tibshirani R, Børresen-Dale AL, Pollack JR. 2006. Distinct patterns of DNA copy number alteration are associated with different clinicopathological features and gene-expression subtypes of breast cancer. Genes Chrom Cancer 45:1033–1040.

Bignell GR, Greenman CD, Davies H, Butler AP, Edkins S, Andrews JM, Buck G, Chen L, Beare D, Latimer C, Widaa S, Hinton J, Fahey C, Fu B, Swamy S, Dalgliesh GL, Teh BT, Deloukas P, Yang F, Campbell PJ, Futreal PA, Stratton MR. 2010. Signatures of mutation and selection in the cancer genome. Nature 463:893–898.

Borrás C, Gómez-Cabrera MC, Viña J. 2011. The dual role of p53: DNA protection and antioxidant. Free Radic Res 45:643–652.

Bottillo I, Ahlquist T, Brekke H, Danielsen SA, van den Berg E, Mertens F, Lothe RA, Dallapiccola B. 2009. Germline and somatic *NF1* mutations in sporadic and NF1-associated malignant peripheral nerve sheath tumours. J Pathol 217:693–701.

Brems H, Beert E, de Ravel T, Legius E. 2009a. Mechanisms in the pathogenesis of malignant tumors in neurofibromatosis type 1. Lancet Oncol 10:508–515.

Brems H, Park C, Maertens O, Pemov A, Messiaen L, Upadhyaya M, Claes K7, Beert E, Peeters K, Mautner V, Sloan J, Yao L, Lee R, Sciot R, De Smet L, Legius E1, Stewart D. 2009b. Molecular pathogenesis of NF1 related glomus tumors. Cancer Res 69:7393–7401.

Bridge RS Jr., Bridge JA, Neff JR, Naumann S, Althof P, Bruch LA. 2004. Recurrent chromosomal imbalances and structurally abnormal breakpoints within complex karyotypes of malignant peripheral nerve sheath tumor and malignant triton tumor: a cytogenetic and molecular cytogenetic study. J Clin Pathol 57:1172–1178.

Cairns P, Polascik TJ, Eby Y, Tokino K, Califano J, Merlo A, Mao L, Herath J, Jenkins R, Westra W. 1995. Frequency of homozygous deletion at p16/CDKN2 in primary human tumors. Nat Genet 11:210–212.

Carroll SL, Ratner N. 2008. How does the Schwann cell lineage form tumors in NF1? Glia 56:1590–1605.

Chen Y, Chen C. 2008. DNA copy number variation and loss of heterozygosity in relation to recurrence of and survival from head and neck squamous cell carcinoma: a review. Head Neck 30:1361–1383.

Cichowski K, Jacks T. 2001. *NF1* tumor suppressor gene function: narrowing the GAP. Cell 104:593–604.

Dear PH. 2009. Copy-number variation: the end of the human genome? Trends Biotechnol 27:448–454.

Ding L, Getz G, Wheeler DA, Mardis ER, McLellan MD, Cibulskis K, Sougnez C, Greulich H, Muzny DM, Morgan MB, Fulton L, Fulton RS, Zhang Q, Wendl MC, Lawrence MS, Larson DE, Chen K, Dooling DJ, Sabo A, Hawes AC, Shen H, Jhangiani SN, Lewis LR, Hall O, Zhu Y, Mathew T, Ren Y, Yao J, Scherer SE, Clerc K, Metcalf GA, Ng B, Milosavljevic A, Gonzalez-Garay ML, Osborne JR, Meyer R, Shi X, Tang Y, Koboldt DC, Lin L, Abbott R, Miner TL, Pohl C, Fewell G, Haipek C, Schmidt H, Dunford-Shore BH, Kraja A, Crosby SD, Sawyer CS, Vickery T, Sander S, Robinson J, Winckler W, Baldwin J, Chirieac LR, Dutt A, Fennell T, Hanna M, Johnson BE, Onofrio RC, Thomas RK, Tonon G, Weir BA, Zhao X, Ziaugra L, Zody MC, Giordano T, Orringer MB, Roth JA, Spitz MR, Wistuba II, Ozenberger B, Good PJ, Chang AC, Beer DG, Watson MA, Ladanyi M, Broderick S, Yoshizawa A, Travis WD, Pao W, Province MA, Weinstock GM, Varmus HE, Gabriel SB, Lander ES, Gibbs RA, Meyerson M, Wilson RK. 2008. Somatic mutations affect key pathways in lung adenocarcinoma. Nature 455:1069–1075.

de Pril R, Perera T, Lekkerkerker A. 2009. A high-content screen for inhibitors of cell migration in cancer metastasis using adenoviral knock-down. Biotech Int 21:16–18.

Erickson HP, Bourdon MA. 1989. Tenascin: an extracellular matrix protein prominent in specialized embryonic tissues and tumors. Annu Rev Cell Biol 5:71–92.

Etienne-Manneville S, Hall A. 2002. Rho GTPases in cell biology. Nature 420:629–635.

Evans DG, Baser ME, McGaughran J, Sharif S, Howard E, Moran A. 2002. Malignant peripheral nerve sheath tumors in neurofibromatosis 1. J Med Genet 39:311–314.

Fang Y, Elahi A, Denley RC, Rao PH, Brennan MF, Jhanwar SC. 2009. Molecular characterization of permanent cell lines from primary, metastatic and recurrent malignant peripheral nerve sheath tumors (MPNST) with underlying neurofibromatosis-1. Anticancer Res 29:1255–1262.

Frahm S, Mautner V, Brems H, Legius E, Debiec-Rychter M, Friedrich R, Knöfel W, Peiper M, Kluwe L. 2004. Genetic and phenotypic characterization of tumor cells derived from malignant peripheral nerve sheath tumors of neurofibromatosis type-1 patients. Neurobiol Dis 16:85–91.

Fritz G, Kaina B. 2006. Rho GTPases: promising cellular targets for novel anticancer drugs. Curr Cancer Drug Targets 6:1–14.

Garcia-Linares C, Fernández-Rodríguez J, Terribas E, Mercadé J, Pros E, Benito L, Benavente Y, Capellà G, Ravella A, Blanco I, Kehrer-Sawatzki H, Lázaro C, Serra E. 2011. Dissecting loss of heterozygosity (LOH) in neurofibromatosis type 1-associated neurofibromas: importance of copy neutral LOH. Hum Mutat 32:78–90.

Gao Y, Xing J, Streuli M, Leto T L, Zheng Y. 2001. Trp^{56} of Rac1 specifies interaction with a subset of guanine nucleotide exchange factors. J Biol Chem 276:47530–47541.

Gao Y, Dickerson JB, Guo F, Zheng J, Zheng Y. 2004. Rational design and characterization of a Rac GTPase-specific small molecule inhibitor. Proc Natl Acad Sci U S A 101:7618–7623.

Glover TW, Stein CK, Legius E, Andersen LB, Brereton A, Johnson S. 1991. Molecular and cytogenetic analysis of tumors in von Recklinghausen neurofibromatosis. Genes Chrom Cancer 3:62–70.

Goh XY, Rees JR, Paterson AL, Chin SF, Marioni JC, Save V, O'Donovan M, Eijk PP, Alderson D, Ylstra B, Caldas C, Fitzgerald RC. 2011. Integrative analysis of array-comparative genomic hybridisation and matched gene expression profiling data reveals novel genes with prognostic significance in oesophageal adenocarcinoma. Gut 60:1317–1326.

Guha A, Lau N, Huvar I, Gutmann D, Provias J, Pawson T, Boss G. 1996. Ras-GTP levels are elevated in human NF1 peripheral nerve tumors. Oncogene 12:507–513.

Harnois T, Constantin B, Rioux A, Grenioux E, Kitzis A, Bourmeyster N. 2003. Differential interaction and activation of Rho family GTPases by p210bcr-abl and p190bcr-abl. Oncogene 22:6445–6454.

Henrichsen CN, Chaignat E, Reymond A. 2009a. Copy number variants, diseases and gene expression. Hum Mol Genet 18:R1–R8.

Henrichsen CN, Vinckenbosch N, Zöllner S, Chaignat E, Pradervand S, Schütz F, Ruedi M, Kaessmann H, Reymond A. 2009b. Segmental copy number variation shapes tissue transcriptomes. Nat Genet 41:424–429.

Hölzel M, Huang S, Koster J, Øra I, Lakeman A, Caron H, Nijkamp W, Xie J, Callens T, Asgharzadeh S, Seeger RC, Messiaen L, Versteeg R, Bernards R. 2010. NF1 is a tumor suppressor in neuroblastoma that determines retinoic acid response and disease outcome. Cell 142:218–229.

International HapMap Consortium. 2005. A haplotype map of the human genome. Nature 437:1299–1320.

John AM, Ruggieri M, Ferner R, Upadhyaya M. 2000. A search for evidence of somatic mutations in the *NF1* gene. J Med Genet 37:44–49.

Kan Z, Jaiswal BS, Stinson J, Janakiraman V, Bhatt D, Stern HM, Yue P, Haverty PM, Bourgon R, Zheng J, Moorhead M, Chaudhuri S, Tomsho LP, Peters BA, Pujara K, Cordes S, Davis DP, Carlton VE, Yuan W, Li L, Wang W, Eigenbrot C, Kaminker JS, Eberhard DA, Waring P, Schuster SC, Modrusan Z, Zhang Z, Stokoe D, de Sauvage FJ, Faham M, Seshagiri S. 2010. Diverse somatic mutation patterns and pathway alterations in human cancers. Nature 466:869–873.

Kanwar JR, Kamalapuram SK, Kanwar RK. 2010. Targeting survivin in cancer: patent review. Expert Opin Ther Pat 20:1723–1737.

Kaempchen K, Mielke K, Utermark T, Langmesser S, Hanemann CO. 2003. Upregulation of the Rac1/JNK signalling pathway in primary human schwannoma cells. Hum Mol Genet 12:1211–1221.

Knudson AG Jr. 1971. Mutation and cancer: statistical study of retinoblastoma. Proc Natl Acad Sci USA 68:820–823.

Kops GJ, Weaver BA, Cleveland DW. 2005. On the road to cancer: aneuploidy and the mitotic checkpoint. Nat Rev Cancer 10:773–785.

Kourea HP, Orlow I, Scheithauer BW, Cordon-Cardo C, Woodruff JM. 1999. Deletions of the INK4A gene occur in malignant peripheral nerve sheath tumors but not neurofibromas. Am J Pathol 155:1855–1860.

Kresse SH, Skårn M, Ohnstad HO, Namløs HM, Bjerkehagen B, Myklebost O, Meza-Zepeda LA. 2008. DNA copy number changes in high-grade malignant peripheral nerve sheath tumors by array CGH. Mol Cancer 7:48.

Kuiper RP, Ligtenberg MJ, Hoogerbrugge N, Geurts van Kessel A. 2010. Germline copy number variation and cancer risk. Curr Opin Genet Dev 20:282–289.

Kuo KT, Guan B, Feng Y, Mao TL, Chen X, Jinawath N, Wang Y, Kurman RJ, Shih IeM, Wang TL. 2009. Analysis of DNA copy number alterations in ovarian serous tumors identifies new molecular genetic changes in low-grade and high-grade carcinomas. Cancer Res 69:4036–4042.

Latres E, Drobnjak M, Pollack D, Oliva MR, Ramos M, Karpeh M, Woodruff JM, Cordon-Cardo C. 1994. Chromosome 17 abnormalities and *TP53* mutations in adult soft tissue sarcomas. Am J Pathol 145:345–355.

LeBron C, Pal P, Brait M, Dasgupta S, Guerrero-Preston R, Looijenga LH, Kowalski J, Netto G, Hoque MO. 2011. Genome-wide analysis of genetic alterations in testicular primary seminoma using high resolution single nucleotide polymorphism arrays. Genomics 97:341–349.

Lee H, Kong SW, Park PJ. 2008. Integrative analysis reveals the direct and indirect interactions between DNA copy number aberrations and gene expression changes. Bioinformatics 24:889–896.

Legius E, Marchuk DA, Collins FS, Glover TW. 1993. Somatic deletion of the neurofibromatosis type 1 gene in a neurofibrosarcoma supports a tumour suppressor gene hypothesis. Nat Genet 3:122–126.

Legius E, Dierick H, Wu R, Hall B, Marynen P, Cassiman J, Glover T. 1994. *TP53* mutations are frequent in malignant NF1 tumors. Genes Chrom Cancer 10: 250–255.

Lévy P, Vidaud D, Leroy K, Laurendeau I, Wechsler J, Bolasco G, Parfait B, Wolkenstein P, Vidaud M, Bièche I. 2004. Molecular profiling of malignant peripheral nerve sheath tumors associated with neurofibromatosis type 1, based on large-scale real-time RT-PCR. Mol Cancer 3:20.

Lévy P, Ripoche H, Laurendeau I, Lazar V, Ortonne N, Parfait B, Leroy K, Wechsler J, Salmon I, Wolkenstein P, Dessen P, Vidaud M, Vidaud D, Bièche I. 2007. Microarray-based identification of tenascin C and tenascin XB, genes possibly involved in tumorigenesis associated with neurofibromatosis type 1. Clin Cancer Res 13:398–407.

Livak KJ, Schmittgen TD. 2001. Analysis of relative gene expression data using real-time quantitative PCR and the 2DDCt method. Methods 25:402–408.

Lothe RA, Slettan A, Saeter G, Brøgger A, Børresen AL, Nesland JM. 1995. Alterations at chromosome 17 loci in peripheral nerve sheath tumors. J Neuropathol Exp Neurol 54:65–73.

Lothe RA, Karhu R, Mandahl N, Mertens F, Saeter G, Heim S, Borresen-Dale AL, Kallioniemi OP. 1996. Gain of 17q24-qter detected by comparative genomic hybridization in malignant tumors from patients with von Recklinghausen's neurofibromatosis. Cancer Res 56:4778–4781.

Lothe RA, Smith-Sørensen B, Hektoen M, Stenwig AE, Mandahl N, Saeter G, Mertens F. 2001. Biallelic inactivation of *TP53* rarely contributes to the development of malignant peripheral nerve sheath tumors. Genes Chrom Cancer 30:202–206.

Maertens O, Prenen H, Debiec-Rychter M, Wozniak A, Sciot R, Pauwels P, De Wever I, Vermeesch JR, de Raedt T, De Paepe A, Speleman F, van Oosterom A, Messiaen L, Legius E. 2006. Molecular pathogenesis of multiple gastrointestinal stromal tumors in NF1 patients. Hum Mol Genet 15:1015–1023.

Malliri A, Collard JG. 2003. Role of Rho-family proteins in cell adhesion and cancer. Curr Opin Cell Biol 15:583–589.

Mantripragada KK, Spurlock G, Kluwe L, Chuzhanova N, Ferner RE, Frayling IM, Dumanski JP, Guha A, Mautner V, Upadhyaya M. 2008. High-resolution DNA copy number profiling of malignant peripheral nerve sheath tumors using targeted microarray-based comparative genomic hybridization. Clin Cancer Res 14:1015–1024.

Mantripragada KK, de Ståhl TD, Patridge C, Menzel U, Andersson R, Chuzhanova N, Kluwe L, Guha A, Mautner V, Dumanski JP, Upadhyaya M. 2009. Genome-wide high-resolution analysis of DNA copy number alterations in NF1-associated malignant peripheral nerve sheath tumors using the 32K BAC array. Genes Chrom Cancer 48:897–907.

Mawrin C, Kirches E, Boltze C, Dietzmann K, Roessner A, Schneider-Stock R. 2002. Immunohistochemical and molecular analysis of p53, RB, and PTEN in malignant peripheral nerve sheath tumors. Virchows Arch 440:610–615.

Miller SJ, Rangwala F, Williams J, Ackerman P, Kong S, Jegga AG, Kaiser S, Aronow BJ, Frahm S, Kluwe L, Mautner V, Upadhyaya M, Muir D, Wallace M, Hagen J, Quelle DE, Watson MA, Perry A, Gutmann DH, Ratner N. 2006. Large-scale molecular comparison of human Schwann cells to malignant peripheral nerve sheath tumor cell lines and tissues. Cancer Res 66:2584–2591.

Miller S, Walter JJ, Mehta T, Hardiman A, Sites E, Kaiser S, Jegga A, Li H, Upadhyaya M, Giovannini M, Muir D, Wallace M, Lopez E, Serra E, Lazaro C, Stemmer-Rachamimov, Page G, Aronow BJ, Ratner N. 2009. Integrative genomic analyses show altered Schwann cell development in neurofibromatosis tumors and implicate *SOX9* as an addicting oncogene. EMBO Mol Med 1:236–248.

Mizuarai S, Machida T, Kobayashi T, Komatani H, Itadani H, Kotani H. 2011. Expression ratio of *CCND1* to *CDKN2A* mRNA predicts *RB1* status of cultured cancer cell lines and clinical tumor samples. Mol Cancer 10:31.

Mullally A, Ebert BL. 2010. *NF1* inactivation revs up Ras in adult acute myelogenous leukemia. Clin Cancer Res 16:4074–4076.

Nielsen GP, Stemmer-Rachamimov AO, Ino Y, Moller MB, Rosenberg AE, Louis DN. 1999. Malignant transformation of neurofibromas in neurofibromatosis 1 is associated with CDKN2A/p16 inactivation. Am J Pathol 155:1879–1884.

Park CH, Rha SY, Jeung HC, Kang SH, Ki DH, Lee WS, Noh SH, Chung HC. 2010. Identification of novel gastric cancer-associated CNVs by integrated analysis of microarray. J Surg Oncol 102:454–461.

Parsons D, Jones S, Zhang X, Lin J, Leary R, Angenendt P, Mankoo P, Carter H, Siu I, Gallia G, Olivi A, McLendon R, Rasheed B, Keir S, Nikolskaya T, Nikolsky Y, Busam D, Tekleab H, Diaz LJ, Hartigan J, Smith D, Strausberg R, Marie S, Shinjo S, Yan H, Riggins G, Bigner D, Karchin R, Papadopoulos N, Parmigiani G, Vogelstein B, Velculescu V, Kinzler K. 2008. An integrated genomic analysis of human glioblastoma multiforme. Science 321:1807–1812.

Perrone F, Tabano S, Colombo F, Dagrada G, Birindelli S, Gronchi A, Colecchia M, Pierotti M, Pilotti S. 2003. p15INK4b, p14ARF, and p16INK4a inactivation in

sporadic and neurofibromatosis type-1-related malignant peripheral nerve sheath tumors. Clin Cancer Res 9:4132–4138.

Perrone F, Mariani L, Pastore E, Orsenigo M, Suardi S, Marcomini B, DaRiva L, Licitra L, Carbone A, Pierotti MA, Pilotti S. 2007. p53 codon 72 polymorphisms in human papillomavirus-negative and human papillomavirus-positive squamous cell carcinomas of the oropharynx. Cancer 109:2461–2465.

Perrone F, Da Riva L, Orsenigo M, Losa M, Jocollè G, Millefanti C, Pastore E, Gronchi A, Pierotti MA, Pilotti S. 2009. *PDGFRA*, *PDGFRB*, *EGFR*, and downstream signalling activation in malignant peripheral nerve sheath tumor. Neuro Oncol 11:725–736.

Qi Y, Huang B, Yu L, Wang Q, Lan G, Zhang Q. 2009. Prognostic value of Tiam1 and Rac1 overexpression in nasopharyngeal carcinoma. ORL J Otorhinolaryngol Relat Spec 71:163–171.

Rajagopalan H, Lengauer C. 2004. Aneuploidy and cancer. Nature 432:338–341.

Rasmussen S, Overman J, Thomson S, Colman S, Abernathy C, Trimpert R, Moose R, Virdi G, Roux K, Bauer M, Rojiani A, Maria B, Muir D, Wallace M. 2000. Chromosome 17 loss-of-heterozygosity studies in benign and malignant tumors in neurofibromatosis type-1. Genes Chrom Cancer 28:425–431.

Rothenberg SM, Settleman J. 2010. Discovering tumor suppressor genes through genome-wide copy number analysis. Curr Genomics 11:297–310.

Sabah M, Cummins R, Leader M, Kay E. 2006. Loss of p16 (INK4A) expression is associated with allelic imbalance/loss of heterozygosity of chromosome 9p21 in microdissected malignant peripheral nerve sheath tumors. Appl Immunohistochem Mol Morphol 14:97–102.

Sangha N, Wu R, Kuick R, Powers S, Mu D, Fiander D, Yuen K, Katabuchi H, Tashiro H, Fearon E, Cho K. 2008. Neurofibromin 1 (NF1) defects are common in human ovarian serous carcinomas and co-occur with *TP53* mutations. Neoplasia 10:1362–1372.

Schmidt H, Taubert H, Meye A, Würl P, Bache M, Bartel F, Holzhausen HJ, Hinze R. 2000. Gains in chromosomes 7, 8q, 15q and 17q are characteristic changes in malignant but not in benign peripheral nerve sheath tumors from patients with Recklinghausen's disease. Cancer Lett 155:181–190.

Schmittgen T, Livak KJ. 2008. Analyzing real-time PCR data by the comparative C_T method. Nat Protocols 3:1101–1108.

Schubbert S, Shannon K, Bollag G. 2004. Hyperactive Ras in developmental disorders and cancer. Nat Rev Cancer 7:295–308.

Serra E, Rosenbaum T, Winner U, Aledo R, Ars E, Estivill X, Lenard HG, Lázaro C. 2000. Schwann cells harbor the somatic *NF1* mutation in neurofibromas: evidence of two different Schwann cell subpopulations. Hum Mol Genet 9:3055–3064.

Shlien A, Malkin D. 2010. Copy number variations and cancer susceptibility. Curr Opin Oncol 22:55–63.

Shlien A, Malkin D. 2009. Copy number variations and cancer. Genome Med 1:62.

Shapiro SD. 1999. Diverse roles of macrophage matrix metalloproteinases in tissue destruction and tumor growth. Thromb Haemost 82:846–849.

Shapiro SD. 1998. Matrix metalloproteinase degradation of extracellular matrix: biological consequences. Curr Opin Cell Biol 10:602–608.

Side L, Taylor B, Cayouette M, Conner E, Thompson P, Luce M, Shannon K. 1997. Homozygous inactivation of the *NF1* gene in bone marrow cells from children with neurofibromatosis type 1 and malignant myeloid disorders. N Engl J Med 336:1713–1720.

Skotheim R, Kallioniemi A, Bjerkhagen B, Mertens F, Brekke H, Monni O, Mousses S, Mandahl N, Soeter G, Nesland J, Smeland S, Kallioniemi O, Lothe R. 2003. Topoisomerase-II alpha is upregulated in malignant peripheral nerve sheath tumors and associated with clinical outcome. J Clin Oncol 21:4586–4591.

Skuse GR, Kosciolek BA, Rowley PT.1989. Molecular genetic analysis of tumors in von Recklinghausen neurofibromatosis: loss of heterozygosity for chromosome 17. Genes Chromosomes Cancer 1:36–41.

Spurlock G, Knight SJ, Thomas N, Kiehl TR, Guha A, Upadhyaya M. 2010. Molecular evolution of a neurofibroma to malignant peripheral nerve sheath tumor (MPNST) in an NF1 patient: correlation between histopathological, clinical and molecular findings. J Cancer Res Clin Oncol 136:1869–1880.

Stasik CJ, Tawfik O. 2006. Malignant peripheral nerve sheath tumor with rhabdomyosarcomatous differentiation (malignant triton tumor). Arch Pathol Lab Med 130:1878–1881.

Stevenson DA, Zhou H, Ashrafi S, Messiaen LM, Carey JC, D'Astous JL, Santora SD, Viskochil DH. 2006. Double inactivation of *NF1* in tibial pseudarthrosis. Am J Hum Genet 79:143–148.

Stewart W, Traynor JP, Cooke A, Griffiths S, Onen NF, Balsitis M, Shah AA, Upadhyaya M, Tobias ES. 2007. Gastric carcinoid: germline and somatic mutation of the neurofibromatosis type 1 gene. Fam Cancer 6:147–152.

Stewart H, Bowker C, Edees S, Smalley S, Crocker M, Mechan D, Forrester N, Spurlock G, Upadhyaya M. 2008. Congenital disseminated neurofibromatosis type 1: a clinical and molecular case report. Am J Med Genet 146A:1444–1452.

Storlazzi CT, Brekke HR, Mandahl N, Brosjö O, Smeland S, Lothe RA, Mertens F. 2006. Identification of a novel amplicon at distal 17q containing the *BIRC5*/SURVIVIN gene in malignant peripheral nerve sheath tumors. J Pathol 209:492–500.

Stratton MR, Campbell PJ, Futreal PA. 2009. The cancer genome. Nature 458:719–724.

Suzuki M, Kato M, Yuyan C, Takita J, Sanada M, Nannya Y, Yamamoto G, Takahashi A, Ikeda H, Kuwano H, Ogawa S, Hayashi Y. 2008. Whole-genome profiling of chromosomal aberrations in hepatoblastoma using high-density single-nucleotide polymorphism genotyping microarrays. Cancer Sci 99:564–570.

Tabone-Eglinger S, Bahleda R, Côté JF, Terrier P, Vidaud D, Cayre A, Beauchet A, Théou-Anton N, Terrier-Lacombe MJ, Lemoine A, Penault-Llorca F, Le Cesne A, Emile JF. 2008. Frequent EGFR positivity and overexpression in high-grade areas of human MPNSTs. Sarcoma 2008:849156.

Tucker T, Wolkenstein P, Revuz J, Zeller J, Friedman JM. 2005. Association between benign and malignant peripheral nerve sheath tumors in NF1. Neurology 65:205–211.

Upadhyaya M, Cooper DN, editors. 1998. Neurofibromatosis Type 1: From genotype to phenotype. Oxford: BIOS Scientific Publishers.

Upadhyaya M, Han S, Consoli C, Majounie E, Horan M, Thomas NS, Potts C, Griffiths S, Ruggieri M, von Deimling A, Cooper DN. 2004. Characterisation of the somatic mutational spectrum of the neurofibromatosis type 1 (*NF1*) gene in neurofibromatosis patients with benign and malignant tumors. Hum Mutat 23:134–146.

Upadhyaya M, Kluwe L, Spurlock G, Monem B, Majounie E, Mantripragada K, Ruggieri M, Chuzhanova N, Evans DG, Ferner R, Thomas N, Guha A, Mautner V. 2008a. Germline and somatic *NF1* gene mutation spectrum in NF1-associated malignant peripheral nerve sheath tumors (MPNSTs). Hum Mutat 29:74–82.

Upadhyaya M, Spurlock G, Monem B, Thomas N, Friedrich RE, Kluwe L, Mautner V. 2008b. Germline and somatic *NF1* gene mutations in plexiform neurofibromas. Hum Mutat 29:E103–E111.

Upadhyaya M. 2010. Neurofibromatosis type 1: diagnosis and recent advances. Expert Opin Med Diagn 4:307–322.

Upadhyaya M. 2011. Genetic basis of tumorigenesis in NF1 malignant peripheral nerve sheath tumors. Front Biosci 16:937–951.

Vahidnia A, van der Straaten RJHM, Romijn F, van Pelt J, van der Voet GB, de Wolff FA. 2007. Arsenic metabolites affect expression of the neurofilament and tau genes: an *in-vitro* study into the mechanism of arsenic neurotoxicity. Toxicol In Vitro 21:1104–1112.

Weir B, Zhao X, Meyerson M. 2004. Somatic alterations in the human cancer genome. Cancer Cell 6:433–438.

Worthylake DK, Rossman KL, Sondek J. 2000. Crystal structure of Rac1 in complex with the guanine nucleotide exchange region of Tiam1. Nature 408: 682–688.

Wu M, Zhi-fen W, Wu, Merajver SD. 2007. Rho proteins and cell-matrix interactions in cancer. Cells Tissues Organs 18:100–103.

Yu J, Deshmukh H, Payton JE, Dunham C, Scheithauer BW, Tihan T, Prayson RA, Guha A, Bridge JA, Ferner RE, Lindberg GM, Gutmann RJ, Emnett RJ, Salavaggione L, Gutmann DH, Nagarajan R, Watson MA, Perry A. 2011. Array-based comparative genomic hybridization identifies CDK4 and FOXM1 alterations as independent predictors of survival in malignant peripheral nerve sheath tumor. Clin Cancer Res 17:1924–1934.

Zheng M, Simon R, Mirlacher M, Maurer R, Gasser T, Forster T, Diener PA, Mihatsch MJ, Sauter G, Schraml P. 2004. *TRIO* amplification and abundant mRNA expression is associated with invasive tumor growth and rapid tumor cell proliferation in urinary bladder cancer. Am J Pathol 165:63–69.